METHODOLOGY FOR IMPLEMENTING FRACTURE MECHANICS IN GLOBAL STRUCTURAL DESIGN OF AIRCRAFT

THESIS

Clifton D. Nees, Captain, USAF

AFIT/GAE/ENY/95D-18

DEPARTMENT OF THE AIR FORCE
AIR UNIVERSITY
AIR FORCE INSTITUTE OF TECHNOLOGY

Wright-Patterson Air Force Base, Ohio

METHODOLOGY FOR IMPLEMENTING FRACTURE MECHANICS IN GLOBAL STRUCTURAL DESIGN OF AIRCRAFT

THESIS

Clifton D. Nees, Captain, USAF

AFIT/GAE/ENY/95D-18

METHODOLOGY FOR IMPLEMENTING FRACTURE MECHANICS IN GLOBAL STRUCTURAL DESIGN OF AIRCRAFT

THESIS

Presented to the Faculty of the School of Engineering

Air Education and Training Command

In Partial Fulfillment of the Requirements for the Degree of

Master of Science in Aeronautical Engineering

Clifton D. Nees, B.S., M.S.

Captain, USAF

December 1995

Acknowledgments

I would like to thank my thesis advisor, Major Robert Canfield, for his guidance throughout my research. His steady support and willingness to listen were greatly appreciated. I would also like to thank my thesis sponsor, Dr. Venkayya from Wright Laboratory, Flight Dynamics Directorate. He not only inspired the subject of my thesis but also helped to maintain a focus on the end use of the research. In addition, I would like to thank Mr. Jim Harter from Wright Laboratory for supplying and supporting the MODGRO computer program used in my thesis. Lastly, I would like to thank my lovely wife, Joanna, for her patience and understanding.

Table of Contents

List of Figures

List of Tables

Abstract

The analysis and design criteria of fracture mechanics is investigated for implementation with the Automated Structural Optimization System (ASTROS) global optimization design tool. The main focus is the optimal design of aircraft wing panels by applying fracture mechanics design criteria within the global finite element model. This effort consists of four main phases: investigation of fracture mechanics analysis methods and design criteria, formulation of a computational technique for damage tolerance design consistent with global optimization requirements, integration of the technique into the ASTROS design tool, and demonstration of the results.

METHODOLOGY FOR IMPLEMENTING FRACTURE MECHANICS

IN GLOBAL STRUCTURAL DESIGN OF AIRCRAFT

I. Introduction

Background

The advent of computational optimization tools has begun to change the way modern aircraft are designed. Recognizing the potential benefits of optimization, the Air Force sponsored the development of the Automated Structural Optimization System (ASTROS) for use by government, academia, and commercial aerospace companies [1]. However, implementing optimization in such a complex and multi-disciplinary problem as aircraft design remains a challenge. As is often the case in computational methods, modeling technique is one of those challenges.

Despite the amazing advances in computer capabilities in recent years, modeling every stringer, rivet, and cutout of an aircraft remains impractical in computational optimization. Therefore, more coarse "global" models are used to optimize the overall aircraft design and more detailed design is conducted after-the-fact. However, if the detailed "local" design cannot be achieved within the global constraints, the original global optimization may be invalidated. This may result in inaccuracies requiring

modification of the global model and a new optimization. Obviously, this is not desirable due to the cost and time factors that are ever-present in today's aircraft programs.

The benefits of incorporating local modeling issues within a global design was first outlined by Venkayya [2]. The more accuracy that can be injected into the global design (without a disproportionate increase in computational requirements), the more easily the local design can be achieved within the global constraints . Therefore, the interaction between local and global design must be investigated to identify design variables that may produce the best increase in accuracy for the least expense. One design issue that plays a large role in both local and global aircraft design is damage tolerance.

"In 1970, the USAF started to develop a Damage Tolerance Philosophy in order to eliminate the type of structural failures and cracking problems encountered on various military aircraft [3:1.1.1] ." This culminated in several USAF military specifications [4,5,6] . Since then, damage tolerance requirements have played an increasing role in aircraft design. The objective of damage tolerance requirements is "to protect the safety of flight structure from potentially deleterious effects of material, manufacturing and processing defects through proper material selection and control, control of stress levels, use of fracture resistant design concepts, manufacturing and process controls and the use of careful inspection procedures [5:1] ." The primary analytical tool throughout the damage tolerant design process is fracture mechanics.

Fracture mechanics is the field of engineering which studies the behavior of a damaged or cracked structure. In recent years, numerical methods (such as: finite element, finite difference, and boundary element) have been brought to bear on fracture mechanics [7] . However, these methods require more detailed modeling than is available in the global model and, therefore, are more applicable to the local design.

The intent of this thesis is to demonstrate the use of conventional fracture mechanics analysis in combination with an aircraft's global finite element model to establish fatigue allowables. Another goal is to evaluate the interaction between the local modeling for fatigue criteria and global design.

Objective

The first objective is to demonstrate a method of linking the ASTROS program to a fracture mechanics prediction code in order to develop fatigue stress allowables for aircraft wing panels. The second objective is to investigate how local modeling of the panels affect the accuracy of the fracture mechanics analysis. A demonstration case will be selected to obtain trends due to the effects of different panel features. The following panel features will be examined: panel location on the wing, panel geometry, panel thickness, material properties, and stiffener configuration. The third objective is to investigate the global design variables and their sensitivity to the fracture mechanics analysis. Thus, possible benefits to including this procedure within a global optimization loop can be identified.

This research is not intended to advance the state-of-the-art of fracture analysis, but rather to identify current capabilities that can be used to make ASTROS global optimization more relevant by satisfying the local fatigue design requirements.

Thesis Organization

This thesis is organized into six chapters: Introduction, Literature Review, Methodology, Results, Recommendations, and Conclusions. This first chapter describes the motivation, objective, and scope of the research. The second chapter provides a short background of general fracture mechanics theory and then focuses on specific aspects of fracture mechanics that pertain to aircraft wing panel design. The third chapter outlines the theory, assumptions, and logic behind the methodology employed in this design research. Using this methodology, an extensive trade study was conducted to investigate the critical parameters in wing panel design. The results and discussion of these trade studies are presented in the fourth chapter. Based on these results, numerous recommendations for implementation in design and further research are presented in chapter five. The last chapter is a brief summary of the most important findings and recommendations.

II. Literature Review

History of Fracture Mechanics

"The earliest recorded investigations into the phenomenon of fracture would appear to be Leonardo da Vinci's study of the variation of failure strength in different lengths of wire of the same diameter [7:2] ." In 1921, Griffith developed the basic equation of fracture from his study of brittle fracture of glass [8:22-23] . However, it wasn't until the mid-1950's that Irwin's linear stress analysis and local plasticity corrections developed the field of study Irwin called "Fracture Mechanics." [9:1] .

In 1971, Hardrath presented a summary of the current fracture and fatigue analysis capabilities relating to aircraft design [10] . He concluded that "Fracture Mechanics analysis procedures...are not yet capable of treating complex structural and loading conditions [10:138] ." Since then, many advances have been made in the field of fracture mechanics, however, the basic framework presented by Hardrath is clearly evident in the current USAF recommended fatigue design methodology [3] . In addition, fatigue analysis still remains a challenging task for the engineering community:

> The determination of the fatigue crack propagation curve is an essential part of the fracture mechanics design approach....but the prediction of fatigue crack propagation characteristics is even less accurate, despite the vast amount of research that has been done on this subject. Yet the developments achieved during the last decade justify a moderate optimism about the possibilities of prediction techniques. [8:260]

Despite the limitations of fatigue analysis, it remains the only tool currently available in the early phases of damage tolerant design. Therefore, a review of the basic equations and procedures of fatigue analysis is presented next to establish the groundwork for the methodology to be employed.

Fracture Mechanics

A crack in a structure can be loaded in three different modes (Figure 1): opening mode, sliding mode, and tearing mode. Mode I is the most significant, especially for the fatigue of shell type structures used in aircraft wing panel design. Therefore, only

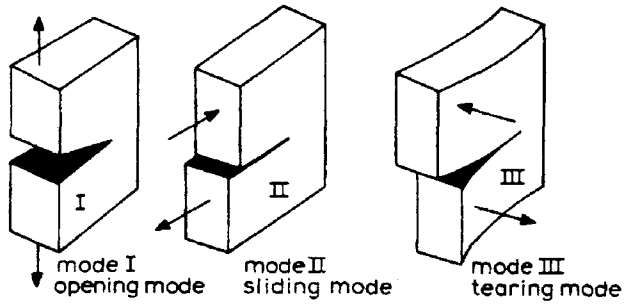

Figure 1: Modes of Stress on a Crack

Mode I will be considered in this research. The *stress intensity factor*, *K*, characterizes the crack tip stress and can be calculated from the following equation:

$$K_I = \beta\sigma\sqrt{\pi a} \qquad (1)$$

where σ is the far field stress, a is the crack length, and β is a dimensionless factor dependent on geometry, crack size, and other factors. A subscript corresponding to the appropriate mode is used to identify the mode of the stress intensity factor. For the case of a center, through crack in an infinite plate, the dimensionless factor β equals one. The stress intensity for this case is often used when normalizing results and is given the symbol K_o. Solutions to specific crack geometries and loadings can be found in reference material [11,12] .

Toughness. Analogous to an ultimate stress, the fracture toughness K_{Ic} of a material is the limit of the stress intensity factor. When the stress intensity factor equals the material fracture toughness, structural failure occurs, therefore:

$$K_{Ic} = \beta\sigma\sqrt{\pi a_c} \qquad (2)$$

where a_c is the critical crack length and σ is the same as in Eq. (1) . If the crack length is equal to or greater than the critical crack size, the crack becomes unstable and will rapidly grow until failure of the structure.

Although fracture toughness is viewed as a material property, caution must be used because it is dependent upon the material stress state (plane stress vs. plane strain) and, therefore, the thickness and cold working of the material.

Residual Strength. The fracture stress of a cracked body is referred to as *residual strength* and can be calculated from Eq. (1) and the definition of fracture toughness:

$$\sigma_c = \frac{K_{Ic}}{\beta\sqrt{\pi a}} \qquad (3)$$

where σ_c is the residual strength, K_{Ic} is the fracture toughness, a is the crack length, and β is a dimensionless factor. The residual strength of a structure can be used as a design criteria in fatigue analysis [13] .

Fatigue Crack Propagation

Constant Amplitude Loading. For a constant amplitude stress and a given material, the crack propagation can be predicted by relating the stress intensity factor to the change in crack length per cycle. Although many equations have been used to represent the *da/dN* vs. *K* relationship, one commonly used equation was proposed by Walker [8:264-265] :

$$\frac{da}{dN} = C\left(K_{\max}(1-R)^m\right)^n \qquad (4)$$

where *da/dN* is the instantaneous change in crack length per cycle, $K_{\max}$ is stress intensity for the maximum stress, *R* is the stress ratio ($\sigma_{min}/\sigma_{max}$), and *C*, *m*, and *n* are material constants.

It is evident in Figure 2 that the relationship between *da/dN* and *K* is not truly linear on the log-log scale as Eq. (4) suggests. Therefore, the Walker equation is often applied to several segments of the curve to better fit the data. It should be noted that

many factors can contribute to the above material constants. When possible, data should be obtained from experimental test results of similar specimens and test environments.

By integrating Eq. (4) from an initial crack length to the critical crack length a crack growth prediction can be calculated. This integration can rarely be performed in closed-form and, therefore, numerical integration techniques must be used.

Variable-Amplitude Loading. In most real-life situations the stress cycling is variable and not a constant amplitude. However, predicting crack propagation with variable-amplitude loading is much more complex. "When fatigue cracks are grown under variable-amplitude loading it is possible for the deformation induced at one amplitude to affect the growth rate at another amplitude [14:357] ." A crack's growth experiences a retardation following tensile overloads and, to a lesser extent, an acceleration following compressive overloads. Numerous models, commonly referred to as retardation models, have been proposed to account for variable amplitude loadings.

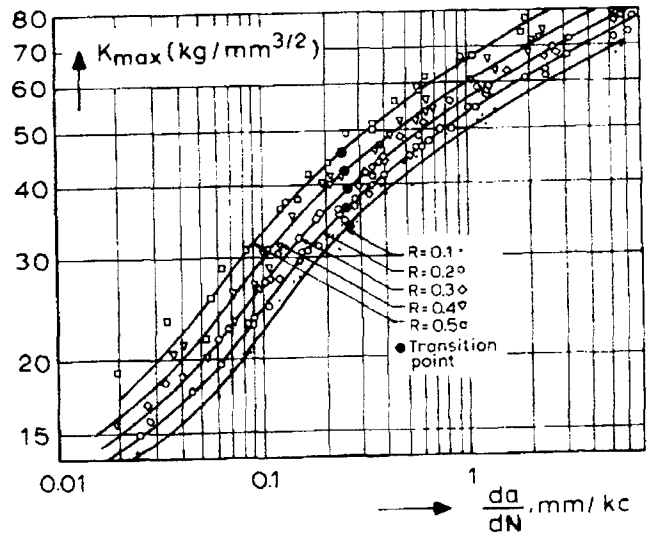

Figure 2: Typical Crack Growth Rate Data [8:264]

Retardation models can be divided into two groups: models based on yield zone size, and models based on closure caused by crack surface deformations that occur within the yield zone. The yield zone models fail to accurately predict the difference between a single tensile overload and a series of multiple overloads. Although the closure models can more accurately predict more varied loading situations (such as multiple overloads), they are more complex and often require simplifications before they can be efficiently utilized [15] .

It is important to understand that the sequence or order of a stress history is immaterial if a retardation model is not used. However, when any retardation model is used, the crack propagation is dependent on the order of the stress history. Therefore, careful thought must be put into the methodology used to sequence the stresses.

Aircraft Design

Aircraft Design Criteria. In 1974, the Air Force defined the damage tolerance design requirements for metallic airframes [5] . The philosophy required that every safety of flight structure be designed for one of two design criteria: slow crack growth or fail-safe. Slow crack-growth structures are designed such that an initial damage will not reach a critical size within a specified period of time. Fail-safe structures rely on redundancy through either multiple-load-paths or crack-arrest structures to maintain flight safety. The slow crack-growth criteria is the primary criteria used in today's Air Force development programs.

The slow crack-growth criteria is specified for two different structure classifications: noninspectable structures, and depot or base level inspectable structures. Each classification has a different set of specifications for initial crack size, growth interval, and residual strength. For noninspectable structures an assumed initial crack size is 1.27 mm (0.05 in) at holes and cutouts or 6.35 mm (0.25 in) for other locations. The initial crack sizes for depot level inspectable structures are larger to account for less accurate inspection techniques: 6.35 mm (0.25 in) at holes and cutouts or 12.70 mm (0.5 in) for other locations. Table 1 lists the growth interval and residual strength required for slow crack-growth structures [16:134-137] .

Aircraft Design Usage. As part of the USAF Aerospace Structural Integrity Program (ASIP), actual in-service usage data of military aircraft have been accumulated [17] . One product of the monitoring program are load-exceedance spectra for different segments of aircraft missions. As seen in Figure 3, the spectrum is defined as the number of times a load factor is exceeded per 1000 flight hours for a given mission segment. Each mission can be described by a sequence of mission segments (Figure 4). Glessler and coworkers [18] outline the methodology for using these load-exceedance

Table 1: Slow Crack-Growth Design Criteria

Inspectability	Safe Crack Growth Interval (lifetimes)	Residual Strength
Depot or base level	0.5	max stress that would occur in 5 lifetimes
Noninspectable	2	max stress that would occur in 20 lifetimes

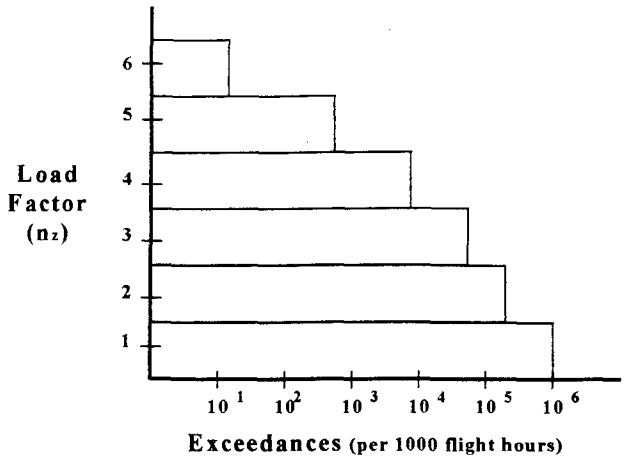

Figure 3: Example Load-Exceedance Spectrum

spectra in combination with aircraft mission profiles to develop an aircraft's design usage. Their guidelines are followed in developing the design usage applied to wing panels in this study.

Aircraft Wing Panels. For most modern aircraft, fatigue criteria play a vital role in the design of wing panels. In the early phases of aircraft development, panel design is

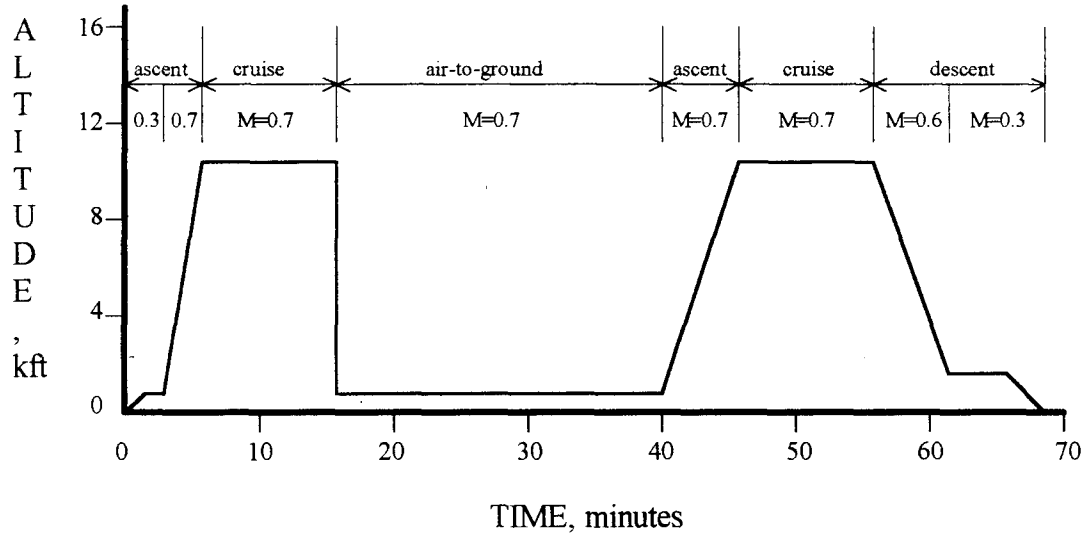

Figure 4: Example Aircraft Mission Profile

usually based on fatigue information from previously developed aircraft. After the preliminary panel design is determined, a damage tolerance analysis is conducted for the "critical" wing panels.

The stresses a critical panel is subjected to throughout its service are determined from the aircraft's design usage and stress analysis. Typically, a stress analysis is conducted on the wing panel for only the most severe maneuvers. The panel stresses for the remaining maneuvers are determined by scaling these results by load factor. A fatigue analysis is then conducted using the panel stresses to determine the *fatigue stress allowable*. If the maximum stress on a panel exceeds the fatigue stress allowable, then local (or maybe even global) design changes are necessary.

The above procedure relies on the ability to identify which wing panels are the "critical" panels. The lower wing panels are more susceptible to fatigue damage because they are subjected to more tensile loading than the upper wing panels. However, past experience has shown that the upper wing panels cannot be ignored. In the early 1980's, unexpected fatigue cracks developed on the upper spar caps of F-15 wings [19] . Investigation revealed that compressive overloads caused residual tensile stresses upon unloading. This example clearly demonstrates that the critical fatigue areas of the wing are not always evident. Therefore, one benefit of linking the fatigue analysis to an aircraft finite element model is the ability to more easily calculate fatigue stress allowables for all wing panels instead of just a select few.

Stiffened Wing Panels. One feature of aircraft wing design that adds complexity to a damage tolerance analysis is stiffened panels. Aircraft wing panels often incorporate

stringers riveted to the wing skin to stiffen the panel. These stringers can have a significant effect on the fatigue behavior of the panel. Poe [20] introduced a method of determining the effect of riveted stringers on the stress intensity of a cracked panel. The rivet loadings are calculated by solving a system of equations which match the displacements of the skin and the stringer at the rivet locations. The stress intensity is then calculated by superposition of the stress intensity from the cracked skin under uniaxial loading and the point loading of each rivet. In this manner, the stress intensity can be calculated as a function of: rivet spacing, stringer spacing, stiffness of the stringer, and crack length.

Swift [21] expanded Poe's approach by incorporating the flexibility of the rivets into the calculation. Swift demonstrated that treating the rivet as rigid results in over-estimation of the stress intensity factor for small cracks and an under-estimation as the crack approaches the stringers.

In their analyses, both Poe and Swift assume the crack propagates between rivet holes instead of propagating from rivet to rivet in a process sometimes called "unzipping." This would appear to be a sweeping assumption considering the close rivet spacing on many aircraft panels. However, the beneficial crack arrest at the hole is counteracted by the acceleration of crack growth toward the hole and the increase of the crack size by the addition of the hole. "Irrespective of the size and spacing of the holes, the crack propagation curve is practically identical to the normal crack growth curve, the differences being in the order of magnitude of the scatter in fatigue crack propagation [8:371] ."

Applications

Since modern damage tolerant design is a recent development in aircraft design, very little literature is available on specific design applications. In addition, there seems to be little consensus in the engineering community concerning the specific details of damage tolerant design procedure. The bulk of publications focus on analysis of specific fatigue failures on existing aircraft designs.

The analysis of the T-39 is one example of fracture mechanics analysis conducted on existing aircraft [22]. The T-39 was designed in the late 1950s and, therefore, preceded the application of current fracture mechanics analysis. However, a full scale fatigue test using a design usage spectrum was conducted to establish a 22,500 flight hour service life. In the mid-1970s, the USAF realized that a substantial portion of the T-39 fleet would exceed their fatigue life capability before the planned retirement of the aircraft. Therefore, a study was initiated to extend the aircraft's service life.

In 1976, the USAF instrumented 10% of the T-39 fleet in order to establish actual aircraft usage data. Using the measured load-exceedance data and a finite element analysis of the wing for the design limit load condition, a damage tolerance analysis was conducted. The results of this analysis were used to establish the required inspection intervals to safely extend the aircraft's service life. Although few details of the analysis were presented in Ref [22], many of the fundamental techniques employed are consistent with the methodology developed in this thesis.

Another example of the application of damage tolerance analysis is the investigation of possible fatigue on the vertical tail of the X-29 due to high tail buffet at high angle-of-attack (aoa) flight [23]. Since the X-29 is an experimental aircraft, the aircraft was not designed using damage tolerance requirements. However, the unexpected buffeting of the vertical tail during high-aoa flight raised the concerns of flight safety during the flight test program. Data obtained from actual in-flight accelerometer measurements on the vertical tail were used to conduct a damage tolerance analysis. The results of the fatigue analysis allowed the completion of the X-29 flight test program by providing a means to safely manage future high-aoa flights. The crack propagation prediction software used in the analysis of the X-29 vertical tail is the same software utilized in this thesis.

III. Methodology

Aircraft design is an extremely complex process involving many multi-disciplinary constraints that must be simultaneously satisfied. However, the majority of these disciplines are often addressed independently with minimal direct interaction with each other. The Automated Structural Optimization System (ASTROS) was specifically developed to facilitate this intricate process of aircraft design. Using ASTROS, a global aircraft design can be optimized based on constraints from numerous different disciplines. In addition, pre-processing modules are constantly being developed for ASTROS to further integrate each discipline's analysis into the global design to reduce redundancy of work and facilitate the flow of data.

One of the more recent design criteria in aircraft design is damage tolerance. If fatigue stress allowables can be estimated early in the design, then they can be used as optimization constraints in a global ASTROS model. The insertion of damage tolerance allowables in the global model should reduce the design difficulties often faced at the local design level.

This chapter outlines a methodology for linking conventional fatigue analysis to a global finite element model to estimate fatigue stress allowables of aircraft wing panels. The methodology was implemented as a software code for demonstration purposes and to investigate sensitivities of the fatigue allowable stresses to certain design variables.

The remainder of this chapter discusses the numerous aspects of a damage tolerance analysis and how they can be applied to the design of aircraft wing panels using information from a global finite element model. After an overview of the methodology, each phase of the analysis is examined in closer detail.

Damage Tolerance Analysis

As in any analysis, many assumptions and intricate details are involved in a damage tolerance analysis. These details can sometimes overshadow the understanding of the overall procedure. Therefore, a brief overview will be presented to establish a framework from which a more thorough discussion can be made.

Any damage tolerance analysis can be separated into two distinct phases: usage analysis and fatigue analysis. The usage analysis is driven by design specifications which outline the intended use of the aircraft. The ultimate result of the usage analysis is a sequence of cyclic stresses (or stress history) which an aircraft component will be subject to throughout its life. The stress history is then normalized by the maximum stress in the sequence. A fatigue analysis is performed on the component based on the component's design and the normalized stress history. The fatigue stress allowable is the largest stress that can multiply the normalized stress history without exceeding the fatigue criteria.

The damage tolerance analysis procedure outlined above was implemented into a software code. Two programs were written to work in conjunction with ASTROS and a

crack growth analysis program called MODGRO [24] . Figure 5 illustrates the data flow between the programs to conduct the damage tolerance analysis.

The computer program, USAGE, is used to define the aircraft's design usage in terms of a sequence of ASTROS load case numbers (load history). The crucial feature of this program is the direct linking of the design usage to a finite element model. Since this design usage is completely independent of panel design, it only needs to be conducted once for all panels.

The second computer program (PANEL) uses as input the aircraft load history and the results of a single ASTROS analysis for multiple load cases. In addition, the user specifies the panel definition, design criteria, material properties, and crack

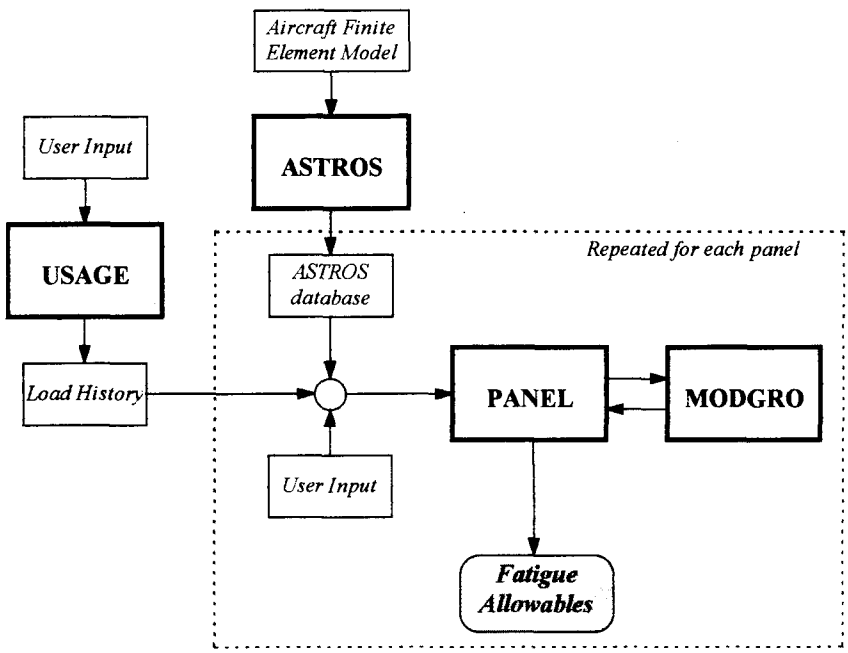

Figure 5: Program Flow

definition. The ASTROS database is used to obtain the panel geometry (length, width, and thickness) and the stresses on the panel for each load case in the load history. These data are used to generate an input file for the crack growth analysis program MODGRO. The MODGRO program is iterated until the fatigue stress allowable is obtained. The fatigue allowable can now be used as a design criterion in the aircraft optimization process.

USAGE Program

The general approach used in the USAGE program follows the guidelines developed by the USAF [18] . Following these guidelines an aircraft's life can be described as a series of flights (usually 1000 hours), blocks of missions, missions, and mission segments as shown in Figure 6. Undoubtedly, this is not the first program developed to create aircraft design usage data by this procedure. However, what sets this

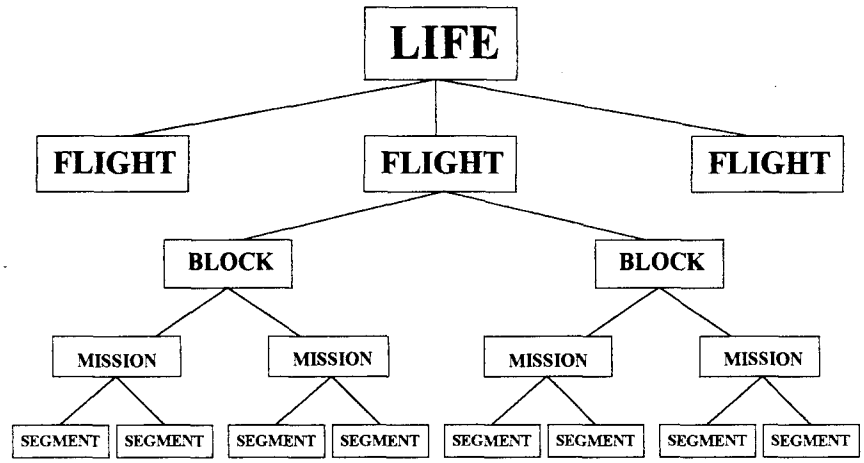

Figure 6: Aircraft Design Usage

program apart is the definition of aircraft maneuvers in terms of ASTROS load cases.

Through the use of ASTROS load case numbers, an aircraft design usage can be converted into wing panel stress histories by directly extracting the stresses from an ASTROS solution database. There are several clear advantages to directly tying the design usage to the global finite element model:

1. Allows fatigue stress allowables to be determined for all wing panels not just a select few.
2. Facilitates the transfer of critical design data (such as: loads, stresses, allowables, etc.) between different design groups involved in the aircraft development.
3. The fatigue analysis can be easily updated as the aircraft's finite element model is refined, changed or optimized.
4. Reduces the difficulties of configuration control throughout the design process.
5. More detailed and accurate stress histories can be developed because any loading that can be modeled in ASTROS can now be easily included in the aircraft's design usage

Mission Profiles. The types of missions an aircraft must perform ultimately defines the design of the aircraft. From the aircraft missions, key design parameters, such as maximum speed, range, endurance, maneuver load factors, and handling qualities are established. Therefore, it should not be surprising that aircraft missions are what define the damage tolerance specifications: severity and frequency of loading.

A mission profile consisting of multiple mission segments (Figure 4) is established for each mission type. Each mission segment is associated with a

Mach/Altitude, flight time, and gross weight (inferred from fuel consumption and weapons release).

Mission Segment. A mission segment is the fundamental building block from which the load history is developed. A load-exceedance spectrum defines the number of times a load factor (n_z) is exceeded in 1000 flight hours of a mission segment. However, each load level of the spectrum can represent any number of maneuver types. Therefore, the number of occurrences in a load level must be split up amongst the different types of maneuvers based on a percentage of their occurrence as illustrated in Figure 7.

Now that the mission segment data has been broken down into individual maneuvers, the maneuvers can be tied to the ASTROS finite element model. A minimum of two parameters are required to uniquely define a maneuver in ASTROS: a boundary condition set and a load case set. In addition, a scaling factor can be specified to scale the stress results of an ASTROS case. For example, the results from a single 9g

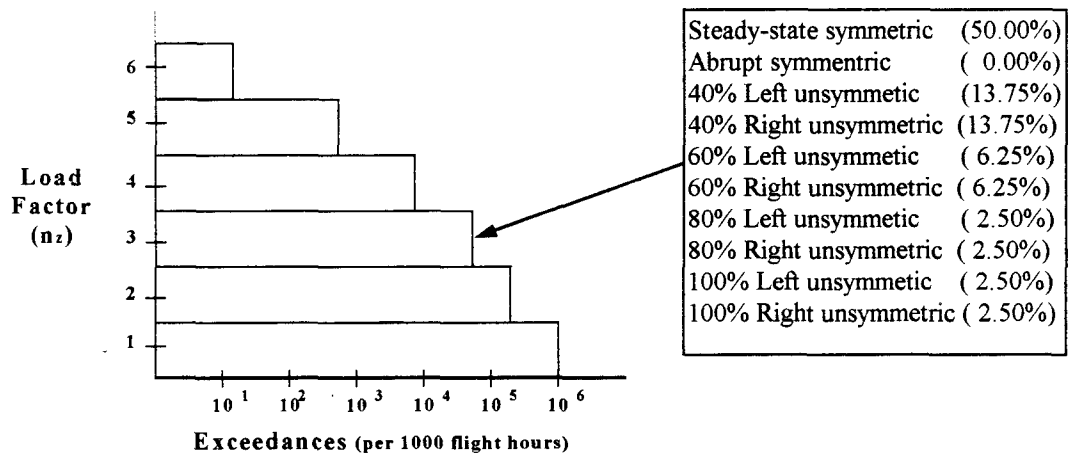

Figure 7: Load-Exceedance Spectrum w/ Maneuver Types

symmetric ASTROS case could be linearly scaled by load factor for each one of the load levels in the spectrum.

The number of maneuvers modeled in ASTROS will undoubtedly be impacted by the damage tolerance analysis. Typically, only a handful of critical maneuvers are modeled for the purpose of aircraft optimization. However, in damage tolerance analysis the greatest number of stress occurrences in the design usage correspond to sub-critical maneuvers. This leads to the conclusion that additional ASTROS cases will be needed to define the maneuvers in the mission segment.

The actual number of maneuvers modeled in ASTROS to adequately define the load history is left to the user to decide. The program is written so that as many (or as few) ASTROS cases can be used to define the mission segments that the user desires. However, for a reasonable amount of accuracy it would be recommend that at least 6 maneuvers for each Mach/Altitude-gross weight combination be used: maximum positive symmetric, maximum negative symmetric, maximum positive unsymmetric (both left and right), and maximum negative unsymmetric (both left and right) [18] . In addition, it would be desirable to include the 1g level flight condition because it occurs so frequently in the load history.

Although the load-exceedance spectrum is tailored to aircraft maneuver data, these spectra can also be used for non-maneuver loads, such as: landing loads, taxi loads, gust loads, etc. Basically, any loading that can be modeled in ASTROS can be assigned

to a load level. The actual value of the load factor assigned to each load level in the USAGE program is primarily for the benefit of the user.

The ability to include diverse loadings in the design usage can be very important in some aircraft design. For example, for transport aircraft with less severe maneuvering envelopes, the gust loadings can become a dominant factor in the fatigue analysis. In the Navy, the carrier landing loads can be significant. In addition, the advent of hypersonic aircraft may present the need for modeling thermal loads as well. In all of these examples, the loadings can be modeled in the same ASTROS finite element model and, therefore, included in the aircraft's design usage.

Load History Sequence. The order of flights, blocks, missions, and segments is defined by user input; however, the actual load cases within each segment are randomly sequenced. A load cycle is created by pairing two randomly selected load cases: one positive (greater than 1g) load factor maneuver and one negative (less than 1g) load factor maneuver. Most exceedance spectra have many more occurrences at positive load factors. Then, 1g maneuvers are used to establish the lower load level of the pairing when negative load factors are exhausted.

Partial Load Occurrences. The mission segment load-exceedance spectra are based on the number of occurrences per 1000 flight hours. However, the flight duration of a particular mission segment during a mission is usually on the order of 1 hour or less. Since the number of load occurrences in each load level is prorated based on the number of flight hours, encountering "partial" load occurrences is likely. Rounding the partial

load occurrences either up or down to an integer value will result in an accumulated error in the number of load occurrences.

In order to minimize the loss of load occurrences, the USAGE program maintains a running total of the partial occurrence for each load level in the mission segments. Each time a mission segment is used in the load history, the partial occurrences are summed. When the summation of a partial occurrences is equal or greater than one, an additional occurrence is added to the load history. Of course, depending on the number of times a mission segment is used in the load history, some partial occurrences may still be lost from the overall load history. For example, a 1 hour mission segment repeated only a few times will be more effected by partial occurrences than a mission segment repeated hundreds of times in the load history.

Repeating and Blocking Data. The number of load cycles in an aircraft's design usage is on the order of millions. This amount of data can produce computational problems: very large data files and very long computation times. Two methods were included in the USAGE program to combat these difficulties: repeating and blocking of the load history data.

The size of the data file can be reduced by simply *repeating* a load history of less flight hours (see Figure 8). For example, a load history representing 1000 flight hours could be repeated 10 times to produce a total of 10,000 flight hours of data. However, load occurrences are lost because the partial occurrences for each mission segment will only be summed up over the 1000 flight hours instead of the entire load history.

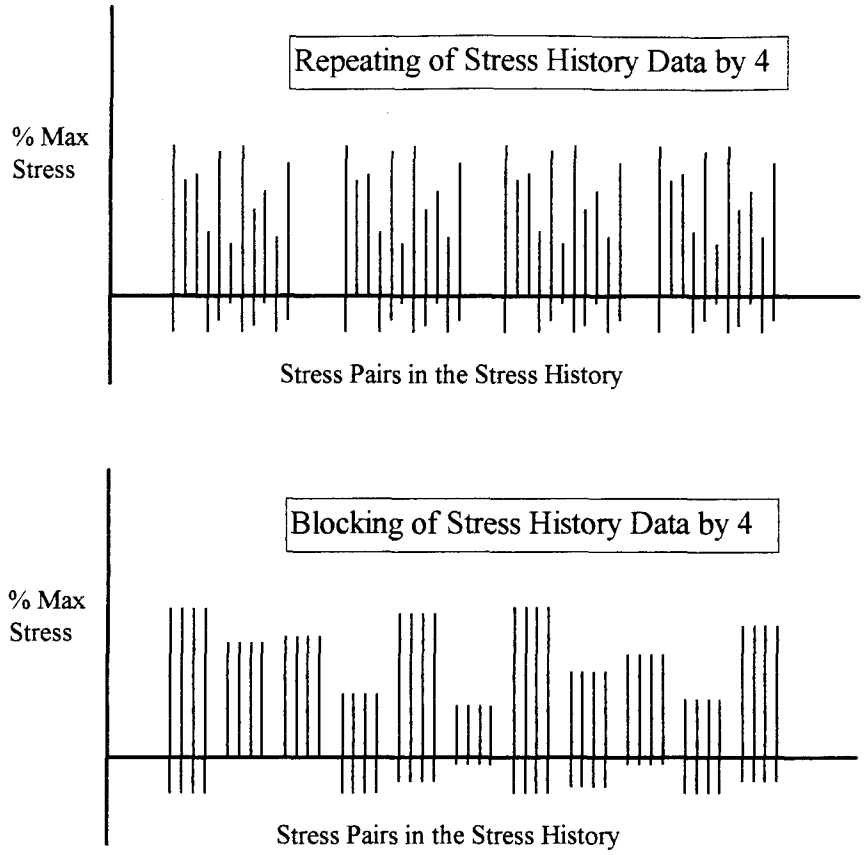

Figure 8: Difference Between Repeating and Blocking the Stress History Data

Although repeating the load history data can easily reduce the size of the data file, it does little to reduce the computation time of the crack propagation integration.

Both the data file size and computation time can be significantly reduced by *blocking* the load history. Instead of repeating the entire load history, each load cycle is repeated within the load history (see Figure 8). For example, each load cycle in a 1000 flight hour load history can be repeated 10 times to produce a 10000 flight hours of data. The repetition of load cycles is referred to as "blocking" in the MODGRO program. This allows the integration to be performed in block size steps instead of cycle size steps. Of

course, this method not only looses load occurrences it also effects the accuracy of the crack propagation if a retardation model is used. The level of inaccuracy is quantified for a particular example in Chapter IV.

PANEL Program

The PANEL program has three primary functions: obtaining panel stress and geometry data from the ASTROS model, producing MODGRO input files in accordance with the user input, and controlling the iteration and convergence of the fatigue stress allowable based on MODGRO output.

ASTROS Panel Information. A pivotal part of the damage tolerance procedure being presented is the use of an ASTROS finite element model to provide stress and panel geometry data. Therefore, the PANEL program must be able to automatically extract the necessary information from an ASTROS solution with a minimum burden on the user. A key feature in ASTROS which will simplify the data transfer is the Computer Aided Design DataBase (CADDB) [25] .

CADDB is a sophisticated relational database which allows ASTROS to operate on extremely large models without exceeding dynamic memory limitations of the computer platform. In addition, it provides an ideal avenue for support programs to read or write data in an ASTROS model. A library of CADDB subroutines is available to perform the basic functions necessary to query and read data from a database. The PANEL program uses these routines to obtain the necessary wing panel information.

The ASTROS finite element model does not distinguish panels of the wing. As far as ASTROS is concerned, the wing is simply a collection of finite elements. An actual panel on the wing can be represented by any number of finite elements depending on the complexity of the model. This difficulty was overcome for local panel buckling constraints in Version 11 of ASTROS by the use of a *master element.*

A single finite element in the model is defined by the user as the master element for a panel. The master element's stress information is assumed to be representative of the entire panel. In addition, the length and width of the panel can be specified. The panel buckling data can be defined in the ASTROS model by the design constraint for buckling (DCONBK) bulk data card. Due to the success of the master element approach in local buckling design, this approach was adopted for the damage tolerance analysis. The user defines a panel in the PANEL program by a designating a single 4-noded quadrilateral (QUAD4) element as the master element. Through the master element, all panel geometry and stress information can be obtained from the ASTROS database.

Panel Stress. The stress intensity factor in Eq. (1) is calculated from the far field stress on the panel. Although the finite element solution produces all components of stress in the master element, what stress should be used to calculate the stress intensity on the crack? This question becomes even more complicated by the fact that a wing panel is subject to non-uniform, biaxial loadings which produce mixed-mode stress intensities (both the opening and sliding modes).

The effect of mixed-mode loading on fatigue crack growth has not been thoroughly studied. "The maximum principal stress criterion postulates that crack

growth will occur in a direction perpendicular to the maximum principal stress [8:375] ." Therefore, the problem is overcome by projecting the crack in the plane of maximum principal stress [7:33] . Indeed, this is supported by mixed-mode testing which demonstrate that an oblique crack will turn at an angle perpendicular to the maximum principal stress angle [8]. From the above tests, it would be tempting to conclude that mixed-mode loadings can be effectively handled by using maximum principal stress to calculate stress intensities. However, these tests were performed with loadings at a constant angle of principal stress. Tests have yet to be performed using more realistic aircraft service loadings where the maximum principal stress direction may change with each load cycle. Although this is the only method currently recommended for mixed-mode fatigue, it needs to be emphasized that it has never been validated for more complex variable loadings.

In the absence of a better method, the PANEL program converts the aircraft load history into panel stress histories by using the maximum principal stress of the panel's master element. The principal stresses are obtained from the element output for the 4-noded quadrilateral element (EOQUAD4) relational database entry. The variation of maximum principal stress angle between different load cases is ignored. This implicitly assumes that the crack propagation can instantaneously change direction to always remain perpendicular to the maximum principal stress. Although this is a questionable assumption, the study of the effects of mixed-mode fatigue is insufficient to provide a better approach.

ASTROS determines the maximum principal stress by selecting the largest algebraic principal stress, not the largest magnitude. If the largest algebraic principal stress is always used, then all compressive wing panel stresses would be virtually ignored. Since compressive stresses accelerate the crack growth, ignoring them would be non-conservative. Therefore, the PANEL program reads both the maximum and minimum principal stress from the ASTROS database and selects the one with the largest magnitude. Another approach considered was using the principal stress nearest the wing's spanwise direction. Although this may more accurately represent an aircraft's wing loading, the maximum magnitude principal stress was used instead because of its conservatism.

Panel Geometry. The master element number is used to query the ASTROS database for the appropriate DCONBK card. From the DCONBK card, both the length and width of the panel are determined. However, if the length and width are not specified in a DCONBK card, then default dimensions are calculated from the master element geometry. The coordinates of the master element grid points are found from the 4-noded quadrilateral element summary table (QUAD4EST) relational entity in the ASTROS database. These coordinates are used to determine the length and width of the panel based on the distance between the midpoints of the sides as shown in Figure 9.

The panel length is assumed to be in the direction of the element's first coordinate axis (defined by ASTROS as the line between the first two nodes). Therefore, the length is calculated as the distance between the midpoints of the two line segments G1G4 and G2G3. Similarly, the width is calculated as the distance between the

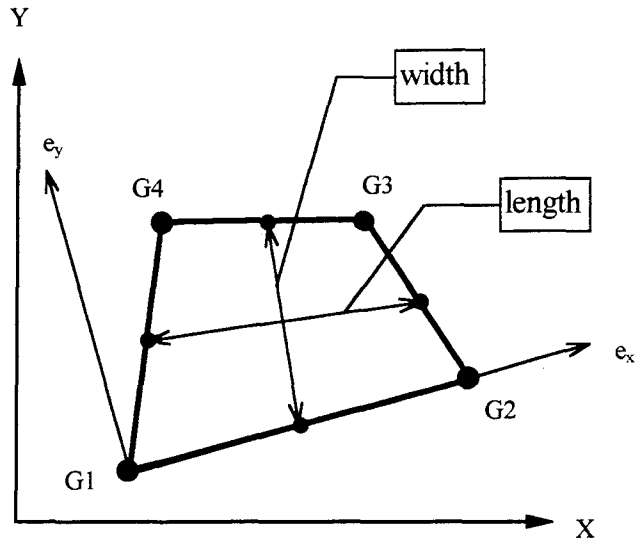

Figure 9: Default Panel Dimensions Based on QUAD4 Geometry

midpoints of the two line segments G1G2 and G3G4. Using the midpoints of the sides produces an average length and width.

The panel thickness is determined from the thickness of the master element. The QUAD4EST database entity is again queried by master element number and the element's center thickness is read from the database.

User Supplied Panel Information. The user must also provide information describing the existing crack in the panel and the material fatigue properties. These data will be used in the MODGRO program to perform the crack propagation analysis. Therefore, the method of specifying this information must be in accordance with the MODGRO input needs.

MODGRO Program. MODGRO is a general purpose crack growth prediction computer program developed by Wright Laboratory. The MODGRO program has a very user-friendly, interactive, graphics interface which simplifies the data input process.

However, for the purposes of this application where the MODGRO program must be interfaced with another program, the graphical interface was unnecessary. Therefore, a batch version of the program was provided by Wright Laboratory for use in this thesis.

Crack Definition. MODGRO contains stress intensity solutions for the most common crack geometries (see Table 2) . These solutions calculate the value of β in Eq. (1) as a function of crack length. In addition to indicating the crack model, the initial crack length must be provided by the user. For surface cracks (1000 series of crack models in Table 2), the following information must be given (see Figure 10): major axis crack length, minor axis crack length, width, thickness, and hole diameter (for cracks emanating from a hole). Through-the-thickness cracks (2000 series crack models in Table 2) have only one crack length and the stress intensity solution does not depend on the panel thickness.

Table 2: MODGRO Stress Intensity Solutions

Crack Model Number	Crack Description
1000	User defined
1010	Center semi-elliptic surface flaw
1020	Center full-elliptic embedded flaw
1030	Single corner crack at a hole
1040	Single surface crack at a hole
1050	Double corner crack at a hole
1060	Double surface crack at a hole
1070	Single edge corner crack
2000	User defined
2010	Center through-crack
2020	Singe through-crack at a hole
2030	Double through-crack at a hole
2040	Single edge through-crack
2050	Double edge through-crack

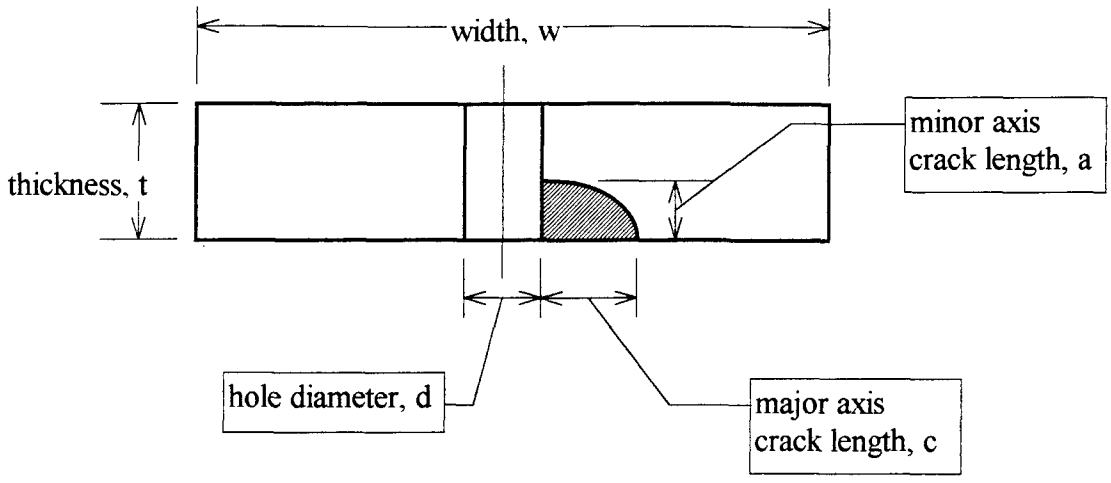

Figure 10: Crack Parameters for Crack Model 1030

Obviously, not all structural cracks can be adequately described by these few models. Therefore, MODGRO provides two methods of handling other crack geometries. The first is through the user definable crack models (models 1000 and 2000). With these crack models, the user must provide tabular data of β vs. crack length (both major and minor axis for surface cracks). The second method allows the user to input tabular data of $\beta_{correction}$ vs. crack length. The $\beta_{correction}$ is a multiplicative correction factor used to scale the β calculated in the specified crack model. This is particularly useful since many references normalize the stress intensity solution by the infinite plate solution (K_o).

Material Fatigue Properties. The crack growth prediction cannot be performed without material fatigue data. Like most material properties, this data must be obtained from material testing. These tests produce data relating da/dN vs. K and R. Since the one of the most common forms of curve fitting this data is the Walker equation,

Eq. (4) , it is included in the MODGRO program. However, MODGRO also allows the fatigue test data to be entered in tabular form. This allows the fatigue properties to be determined through linear interpolation instead of forcing the test data into a curve fit like the Walker equation.

Design Criterion. The design criteria used in the PANEL program to establish the fatigue stress allowable is based on the slow-crack growth criterion established by the USAF. The criterion is that the initial crack will not reach a critical size within a specified period of time. The user specifies the period of time as a multiplication factor of the design usage or life of the aircraft. The number of stress cycles the crack must sustain is calculated by the PANEL program from the number of cycles in the stress history and the multiplication factor. The critical crack size is assumed to be at fracture unless the user designates otherwise.

Iteration and Convergence. As illustrated in Figure 5, the PANEL program creates an input file for the MODGRO program. One item in the input file is the stress multiplication factor which is used in the MODGRO program to scale the normalized stress history. The MODGRO program is executed and the output is read by the PANEL program. If the number of cycles to the critical crack length satisfies the design criteria, then the stress multiplication factor is the fatigue stress allowable. If the number of cycles is too large or too small, then the stress multiplication factor must be adjusted and the crack propagation recomputed.

The method used to select the subsequent stress multiplication factors can drastically effect the number of iterations required to reach convergence. The first guess

is somewhat arbitrary, but it should be reasonable. Therefore, the PANEL program uses the yield stress of the material divided by two as the first guess. For the following iterations the stress multiplication factors are predicted based on the previous iteration's results. The stress multiplication factor versus number of cycles to failure are fit to a power curve using the least-squares method. For the second iteration, an exponent of four is assumed because there are not enough data points to produce a curve fit. Of course, the closer the data matches an exponential curve the more quickly the solution will converge to the design criterion.

As in many computational methods, the question is how close is close enough? Who better to decide the required accuracy than the user? Therefore, the PANEL program allows the user to determine the percentage error from the design criterion. For added flexibility, both the percentage error above (upper tolerance) and below (lower tolerance) the number of stress cycles can be specified. The PANEL program will attempt to converge to the center of the two tolerances.

IV. Results

A significant part of this thesis was the development of a methodology that can be applied to damage tolerant design using a global aircraft finite element model. Although software development was not the objective of this thesis, the implementation of this methodology as a computer program was essential because it permitted further examination of the damage tolerant design issues. Through the use of this software, trade studies were performed to identify the critical design variables. These results can be used to focus further research in the area of damage tolerant design of aircraft.

A finite element model of an F-16 fighter aircraft was selected as the demonstration case for the trade studies. Wing panel features were independently varied to establish their effect on the overall aircraft design. Throughout these trade studies, the percentage change in fatigue stress allowable was used as the figure of merit. This is consistent with aircraft design because a change in the stress allowable has a direct effect on aircraft weight which is the most critical design parameter. In addition, using the same figure of merit for all of the design variables permitted direct comparison of their effects on the design.

Every aircraft design is unique and, therefore, the results from the trade studies on the demonstration case cannot be directly applied to other designs. However, the relative magnitudes of these trades do provide fundamental insight into damage tolerant design of aircraft wing panels. These data can be used to establish research and design priorities concerning wing panel design.

The remainder of this chapter presents the results of numerous different trade studies using the F-16 wing panels and loads, including: design usage data, material properties, panel geometry, stiffened panel design, and the variation of stress distribution. However, a test case was first performed to validate the software.

Test Case

A test case was developed to verify the functionality of the programs. The purpose of the test was to demonstrate the proper flow of data between the programs, as well as confirms that the iteration process can converge to a correct fatigue allowable stress. In order to compare the results to hand calculations, the test case had to be simple enough that a closed-form solution was possible. Therefore, a constant amplitude stress history and integer exponents for the fatigue properties in Eq. (4) were used:

$$\frac{da}{dN} = C\left(K_{\max}(1-R)^m\right)^n$$

where: $C = 1.0(10^{-9})$
R=½
$m = 1$
$n = 4$
$K_{\max}$ is in ksi-in^{½} and da/dN is in in/cycles

For a through-the-thickness crack in an infinite plate and the above assumptions, Eq. (4) can be integrated in closed-form:

$$N = \frac{16 \cdot 10^9}{\sigma_{\max}^4 \, \pi^2}\left(\frac{1}{a_i} - \frac{1}{a_c}\right) \qquad (5)$$

where N is the number of cycles until catastrophic failure, σ_{max} is the maximum stress (ksi), a_i is the initial crack length (in), and a_c is the critical crack length (in). Solving Eq. (3) for critical crack length and substituting the result into Eq. (5) yields:

$$N = \frac{16 \cdot 10^9}{\sigma_{max}^4 \, \pi^2} \left(\frac{1}{a_i} - \pi \left(\frac{\sigma_{max}}{K_{Ic}} \right)^2 \right) \qquad (6)$$

where K_{Ic} is the fracture toughness (K_{Ic} = 45 ksi-in$^{1/2}$ for the test case).

A finite element model was created in ASTROS consisting of a single QUAD4 element under uniform, uniaxial stress. The USAGE program was used to generate the constant amplitude load history with 1 million cycles. The PANEL program was executed to determine σ_{max} for a quarter inch, through-the-thickness, center crack in an infinite plate. The design criteria was one times the design usage before failure (N=10^6 cycles) with a convergence tolerance of ±1% on the number of cycles. The iteration successfully converged to a 998,163 cycles with a fatigue stress allowable of 10.610 ksi.

This result can be checked against the hand calculations by setting the σ_{max} in Eq. (6) to the fatigue stress allowable and calculating the number of cycles, N. For σ_{max}=10.610 ksi, the number of cycles is 1,001,067. Therefore, the number of cycles calculated by the MODGRO program is only 0.29% from the hand calculations. This is a very small amount of error considering the integration in MODGRO is computed according to a cycle-by-cycle numerical procedure.

Description of Demonstration Case

Finite Element Model. An existing ASTROS finite element model of an F-16 aircraft [26] was selected as the demonstration case. "The F-16 is a multinational, multirole fighter aircraft. It performs a wide range of missions necessitating carriage of heavy stores for air-to-ground scenarios and high g maneuvers for air-to-ground scenarios and high g maneuvers for air-to-air maneuvers [26:7] ." The model was selected primarily because the modeling details of the wing box are consistent with the level of detail typically found in a global optimization model (see Figure 11). In fact, the model was originally created for a wing skin optimization study. In addition, multiple load cases were available and well documented.

The finite element model included the six load conditions listed in Table 3. The load cases represent critical design loads for the F-16C wing. Although limited in Mach/Altitude and weapons configurations, the load cases are a good mixture of maneuver types including symmetric and unsymmetric maneuvers at both positive and negative load factors.

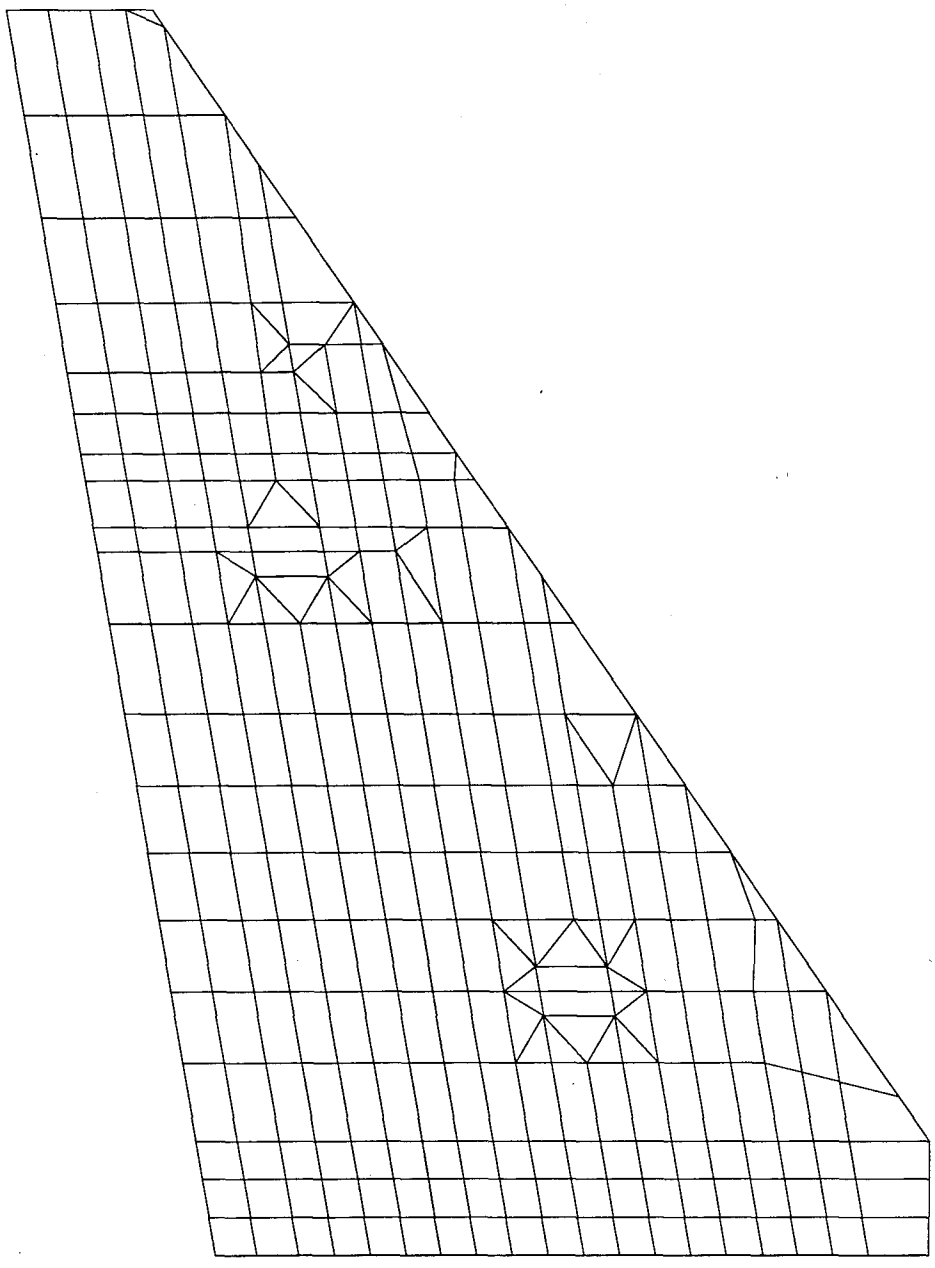

Figure 11: Finite Element Model of the F-16 Lower Wing Skin

Table 3: Selected F-16C Design Load Conditions

Load Case	Critical Component	Maneuver Type	Mach	Altitude
105	Wing	9g Balanced Symmetric Pull-Up	0.95	Sea Level
106	Wing	-3g Balanced Symmetric Push-Over	1.20	Sea Level
107	Flaperon	5.86g 360° Roll	1.20	Sea Level
108	Leading-edge Flap (LEF)	8.58g Balanced Symmetric Pull-Up LEF 21°	0.80	15,000 ft
109	Wing	-1g 180° Roll	1.05	Sea Level
113	Wing Hardpoints	-1g 180° Roll with 3 CBU-58 stores at Hardpoints	0.95	2,500 ft

In the global model, the finite elements are not grouped or identified with individual wing panels. However, the ASTROS design study which used this model did define wing thickness design variables as groups of finite elements. These design variables were adopted as wing panels for this thesis. Figure 12 illustrates the wing panels on the lower wing that were used in the demonstration case.

It is important to understand that the intention is not to conduct an accurate damage tolerance analysis for the actual F-16 aircraft. Rather, the objective is to use this demonstration case as a realistic global model to investigate the behavior of damage tolerance analysis as it pertains to aircraft wing panel design. Therefore, it is more important that the wing panel features examined in this study are indicative of typical

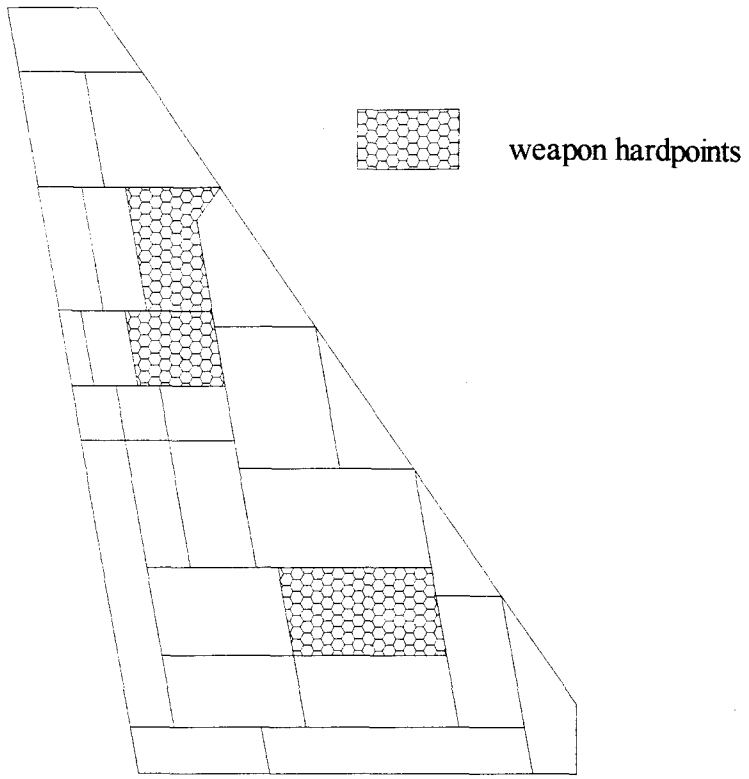

Figure 12: Assumed Panels for Lower Wing Skin for Demonstration Case

aircraft design and less important that it accurately represents the F-16 aircraft represented by this particular model.

Design Usage. The number of maneuvers available in the demonstration model are insufficient to accurately represent the true design usage of the F-16. However, the diverse maneuver types in Table 3 can be used to develop a design usage realistic enough for this study. Since the load cases are the critical design conditions for the F-16 wing, they represent the extremes in different loading situations. Therefore, these few load cases should sufficiently demonstrate the variation in stresses in the wing at different flight conditions.

Given the limited Mach/Altitude conditions available in the model, it was futile to develop a design usage based on a complex arrangement of blocks, missions, and mission segments as shown in Figure 6. Therefore, a composite load-exceedance spectrum was used to develop the design usage (see Figure 13). The composite load-exceedance spectrum is based on an average of all load-exceedance spectra for aircraft in the fighter and attack categories.

Each load level in the cumulative load-exceedance spectrum was defined in terms of one or more of the six load cases and scaled by the load factor. When there was more than one load case for a maneuver, the occurrences were split evenly among them. For example, positive symmetric maneuvers were split between load cases 105 and 108 in Table 3.

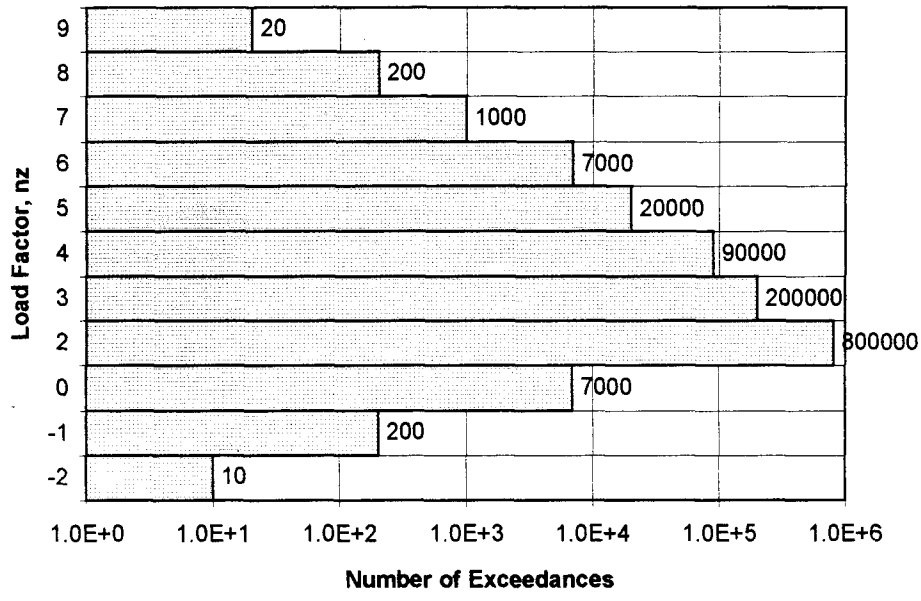

Figure 13: Composite Load-Exceedance Spectrum for Fighter Aircraft [3:5.3.2]

Reference [18] indicates that for fighter/attack aircraft roughly 50% of the maneuvers are symmetric while the other 50% are divided between left and right unsymmetric maneuvers. However, the flight envelope of the F-16 aircraft limits unsymmetric maneuvers to between 5.86g and -1g and, therefore, only symmetric maneuvers were included in occurrences above and below these load factors. In addition, stresses from right rolling maneuvers were assumed to be 50% of the left rolling maneuvers in the demonstration model.

Using the USAGE program and the design usage information discussed above, a 10,000 flight hour load history was developed. Since the design usage is defined in terms of ASTROS load cases, it applies to all wing panels. Therefore, this load history was used as the basis for all of the trade studies to follow.

Design Criteria. The slow crack-growth design criteria for noninspectable structures was used for the wing panel design studies. As shown in Table 1, this criteria requires that the panel must sustain a stress history equivalent to twice the life of the aircraft while maintaining a residual strength greater than the maximum stress that would occur in 20 lifetimes. Since the load cases in the demonstration model are the critical design load cases, the maximum panel stress from these load cases was used as the residual strength regardless of whether it occurred in the load history.

Unless otherwise stated, the initial crack was assumed to be a 6.35 mm (0.25 in) center through-crack in an infinite plate. The crack length is consistent with the noninspectable slow-crack growth criteria. In addition, the crack geometry has the simplest fracture mechanics solution and requires no panel dimensions. Although this is

an over-simplification of an actual wing panel, it provides an ideal baseline from which to make design study variations.

Material Properties. The Walker equation (Eq. (4)) was used to represent the material's fatigue properties. Although the Walker equation is typically applied to several segments of the *da/dN* vs. *K* curve, only one segment was used to facilitate trade studies involving the fatigue properties. Typical values for the fatigue properties of aluminum were obtained from data presented in Ref 27:

$$\frac{da}{dN} = C\left(K_{\max}(1-R)^m\right)^n$$

where: $C = 3.5(10^{-10})$
$m = -0.3$
$n = 3.8$
$K_{\max}$ is in ksi-in$^{1/2}$ and *da/dN* is in in/cycles

and,

$K_{Ic} = 45.0$ ksi-in$^{1/2}$
$K_{th} = 4.0$ ksi-in$^{1/2}$
$\sigma_y = 66.0$ ksi

Figure 14 illustrates the fatigue properties used in this study. Fatigue property curves typically have more of an "S" shape where the data approaches the asymptotic limits of the threshold and critical stress intensities.

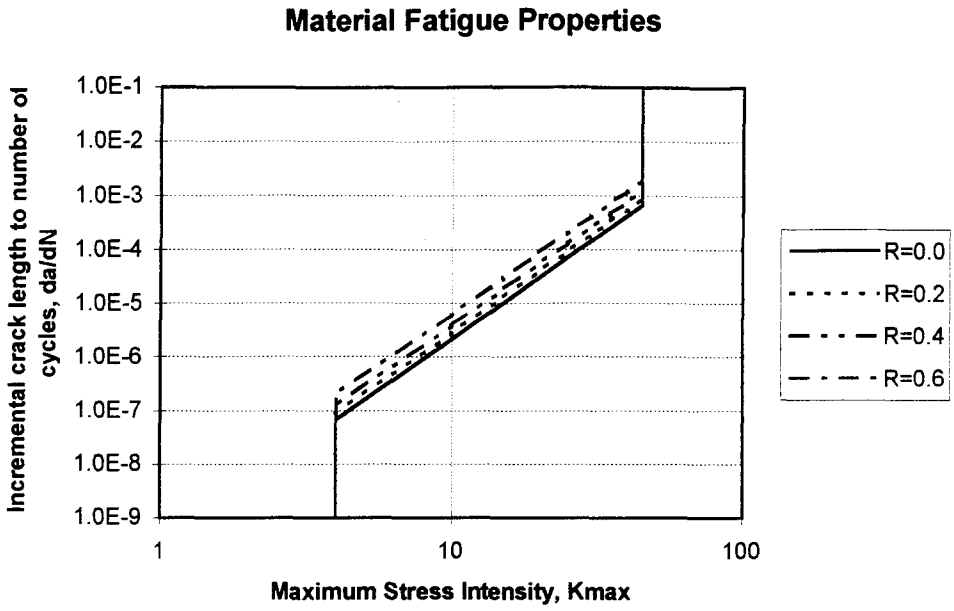

Figure 14: Assumed Fatigue Material Properties

The Willenborg model [8:279-281] was used as the retardation model in this study. In this model, a parameter can be specified which defines the magnitude of the peak stress ratio required to cause crack growth shut-off. This parameter is called the *shut-off ratio* and generally varies between 2.0 and 3.0. Therefore, a value of 2.5 for the shut-off ratio was selected as the baseline for the trade studies.

Wing Panel. A wing panel near the wing root was selected for the baseline case in the trade studies. A wing root panel was chosen because they are typically the focus of attention in most damage tolerance analysis. Figure 15 illustrates the location of the panel selected. This wing panel is modeled as twelve quadrilateral finite elements in the ASTROS model (see Figure 16). A finite element near the panel's center (#2549) was selected as the panel's master element. Therefore, the panel stress history will be

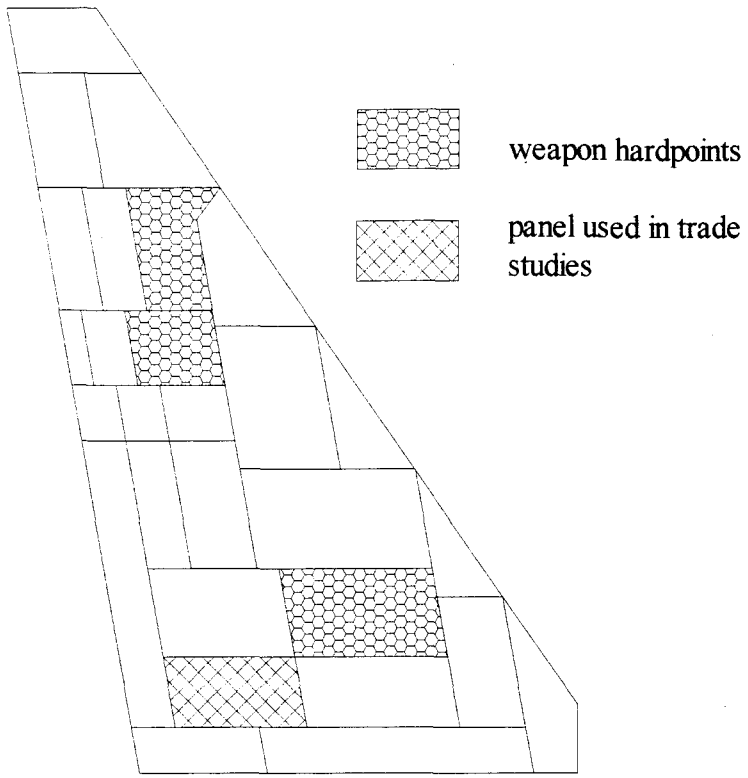

Figure 15: Wing Panel Selected for Trade Studies

determined solely on the finite element solution for element 2549. The principal stress of element 2549 for the six load cases in the finite element model are listed in Table 4.

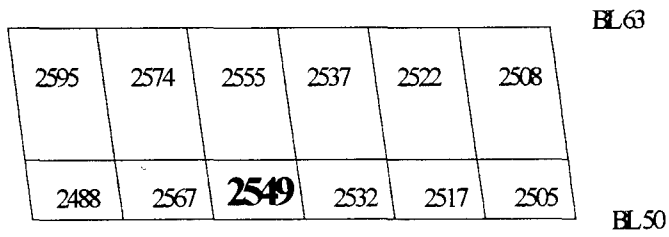

Figure 16: Finite Elements in the Wing Root Panel
(Panel Master Element in Bold)

Table 4: Principal Stresses for Element 2549

ASTROS Load Case	Maximum Principal Stress (ksi)	Minimum Principal Stress (ksi)	Angle of Maximum Principal Stress (deg)
105	32078.7	3189.0	1.365
106	-1249.0	-11361.9	86.523
107	17858.9	1575.6	-8.269
108	25616.9	2649.3	-0.889
109	-564.7	-10051.9	-77.347
113	5345.0	-5822.8	40.427

Design Trade Studies

Blocking & Repeating. The load-exceedance spectrum in Figure 13 has 800,000 cycles that exceed 1g in 1000 flight hours. Therefore, a 10,000 flight hour load history would have 8 million load cycles. With the design criteria of two lifetimes, this becomes a total of 16 million load cycles! As discussed earlier, the load history data can be blocked and/or repeated to reduce file size and computation times. Repeating refers to the repetition of the load history file and blocking is the repetition of each load cycle defined in the load history file. However, what price must be paid for these advantages? The effect of repeating and blocking on the fatigue stress allowable was investigated for the demonstration case.

The effect on the calculated fatigue stress allowable due to repeating and blocking the load history data is presented in Table 5. The small effect of repeating a smaller load history file was expected. The decrease in accuracy due to repeating the load history was less than 1% for repetitions of 1000 or less. The error in the fatigue stress allowable did not become significant (about 5%) until the load history was repeated 10,000 times. The full load history file contains 8 million load cycles (304 MBytes of disk storage) and is reduced linearly with repeating. In this case, the load history was reduced down to a sequence of only 792 load cycles repeated 10,000 times. Although the results cannot be directly applied to all situations because of the variation in design usage development, it does clearly show that a small loss of load cycles due to the repetition of a load history does not significantly effect the results of a damage tolerance analysis. Therefore, if computer resources are limited, the load history file size can be safely reduced through repeating the data.

Table 5: Results for Blocked and Repeated Load Histories

Number of Times the File is Repeated	Number of times the load cycles are blocked	Lost Load Cycles		Fatigue Stress Allowable		CPU Time for Last Iteration
		# lost	%lost	ksi	%change	seconds
1	1	0	0.0%	14.950	0.000%	4874.4
10	1	40	0.0003%	14.963	0.087%	3787.7
100	1	400	0.0025%	14.973	0.154%	3654.3
1,000	1	8,000	0.0500%	15.032	0.548%	3572.0
10,000	1	160,000	1.0000%	15.705	5.050%	3538.6
1	10	40	0.0003%	14.857	-0.622%	489.5
1	100	400	0.0025%	14.558	-2.622%	48.4
1	1,000	8,000	0.0500%	14.250	-4.682%	4.9
1	10,000	160,000	1.0000%	14.480	-3.144%	0.5
10	10	400	0.0025%	14.857	-0.622%	395.9
10	100	8,000	0.0500%	14.603	-2.321%	38.8
10	1,000	160,000	1.0000%	14.624	-2.180%	3.9
100	10	8,000	0.0500%	14.916	-0.227%	377.3
100	100	160,000	1.0000%	14.940	-0.067%	36.1

The results of reducing the load history into blocks of constant amplitude load cycles were more surprising. The error in the fatigue stress allowable was less than 5%. In addition, computation times were reduced roughly linearly with the number of times the load file was blocked (see Table 5). This was offset somewhat by the fact that more iterations were required for convergence as the blocking was increased. Although 5% error is probably unacceptable for the final design allowables, these results do suggest that blocking the load history data could reduce calculation times by orders of magnitude for a quick estimation of the fatigue stress allowables in earlier phases of the aircraft development.

The effects of blocking the data depend not only on the load history, but also on the retardation model used. Since the Willenborg retardation model is a yield criteria model, it is less effected by the multiple overloads that are artificially created by blocking the data. Therefore, other retardation models (especially closure criteria models) may produce different results. However, these data do show that blocking the load history data can be a valuable method of reducing computation times, especially in earlier phases of design when only approximate result are needed.

Another observation that can be made from the above results is the sign of the error for blocked and/or repeated load histories. Repeating the load history file caused an increase in the calculated fatigue stress allowable while blocking the data reduced the fatigue stress allowable. Therefore, blocking the load history file would produce a conservative result (at least with the Willenborg retardation model). In addition, the effects of blocking and repeating tended to counteract each other when used in

combination, as can be seen by comparing rows in Table 5 where the number of lost load cycles are the same.

Due to limited file storage available for this study, a load history repeated 10 times was used for all remaining trade studies. Despite the obvious advantages of reducing computation times, the load history was not blocked to avoid any possible adverse effects.

Material Properties.

Fatigue Slope. The slope of the *da/dN* vs. *K* curve (*n* in the Walker equation) was varied from +30% to -30% of the nominal value. The change in fatigue stress allowable from the allowable for the original slope is shown in Figure 17. As

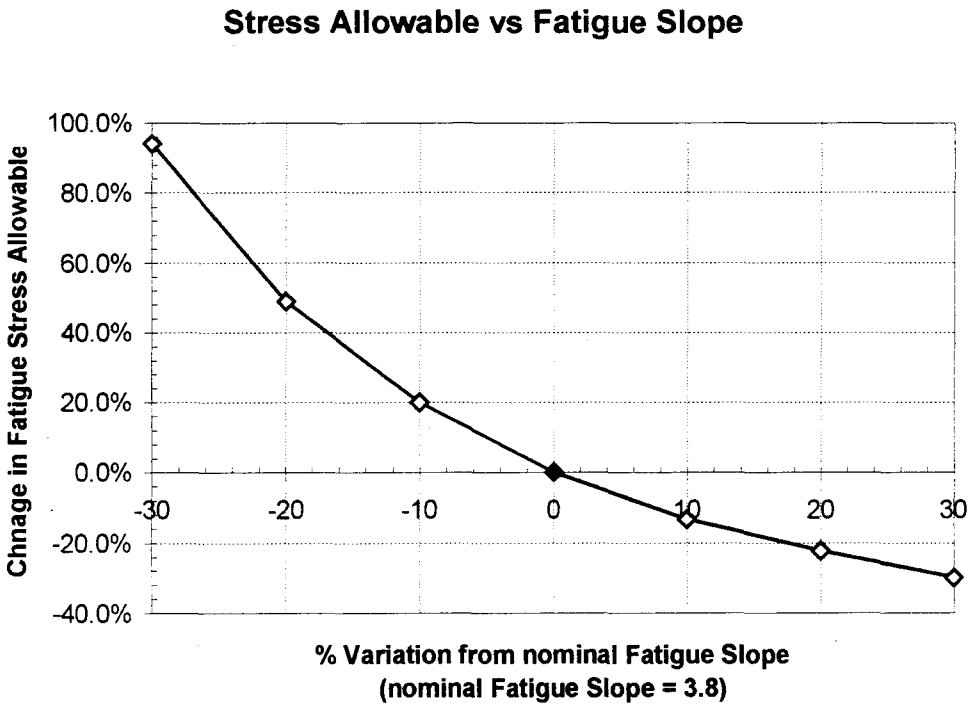

Figure 17: Effect of Fatigue Slope on Fatigue Stress Allowable

expected, the fatigue stress allowable displayed a high sensitivity to the slope of the Walker equation. Obviously, results like these justify the intense amount of research that has been conducted to accurately characterize the fatigue properties of a material.

Toughness. The toughness of a material (K_{Ic}) determines the level of stress intensity a materiel can sustain before catastrophic failure. The material toughness was varied from +30% to -30% of the nominal value. Figure 18 demonstrates that the material toughness actually has little effect on the fatigue stress allowable. The reason for the low sensitivity is that the majority of the stress cycles occur when the crack is very small. By the time the crack is approaching the point of instability, the crack propagation rate is very high. Therefore, the increase or decrease in the number of stress cycles due to a change in the material toughness is small relative to the number of stress cycles that occurred at the smaller crack sizes.

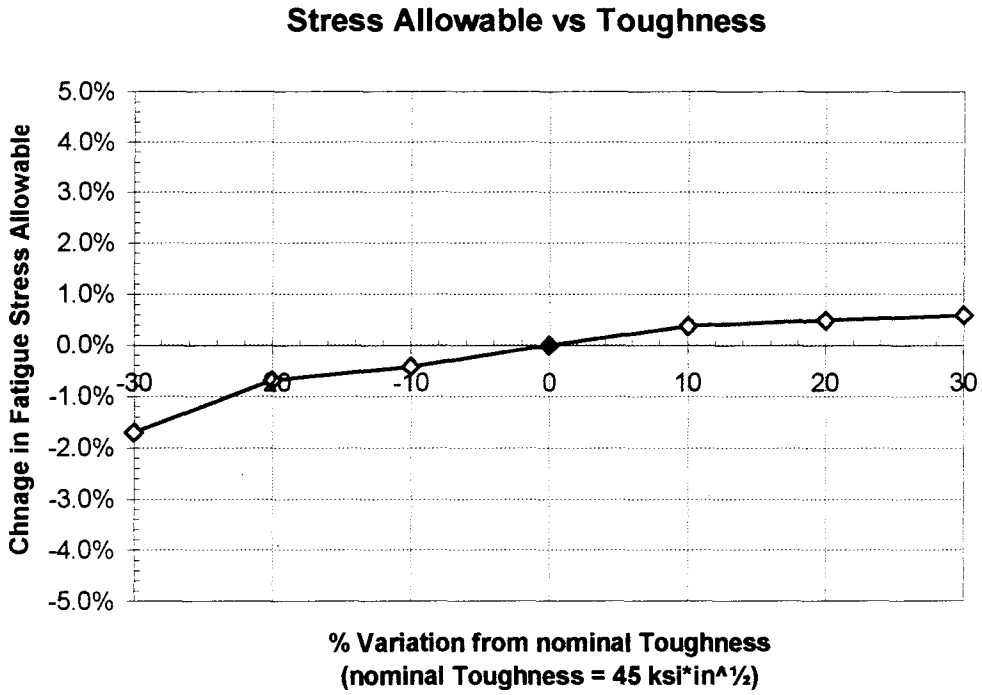

Figure 18: Effect of Toughness on Fatigue Stress Allowable

Willenborg Retardation Shut-Off Ratio. The effect of retardation on the fatigue stress allowable was investigated by varying the Willenborg retardation shut-off ratio. The shut-off ratio was varied from 2 to 3 and the resulting fatigue stress allowables were compared to the result using no retardation. Figure 19 demonstrates that the use of a retardation model can have a significant effect on the crack propagation calculations. However, these results would be even more significant for a less severe stress history than observed for this fighter aircraft. The effect of retardation on a crack propagation increases when the stress history contains many low stress cycles and only a few extremely high stresses.

Panel Geometry. Up to this point, the wing panel has been assumed to be an infinite plate. When the plate is considered to have finite width and length, the stress

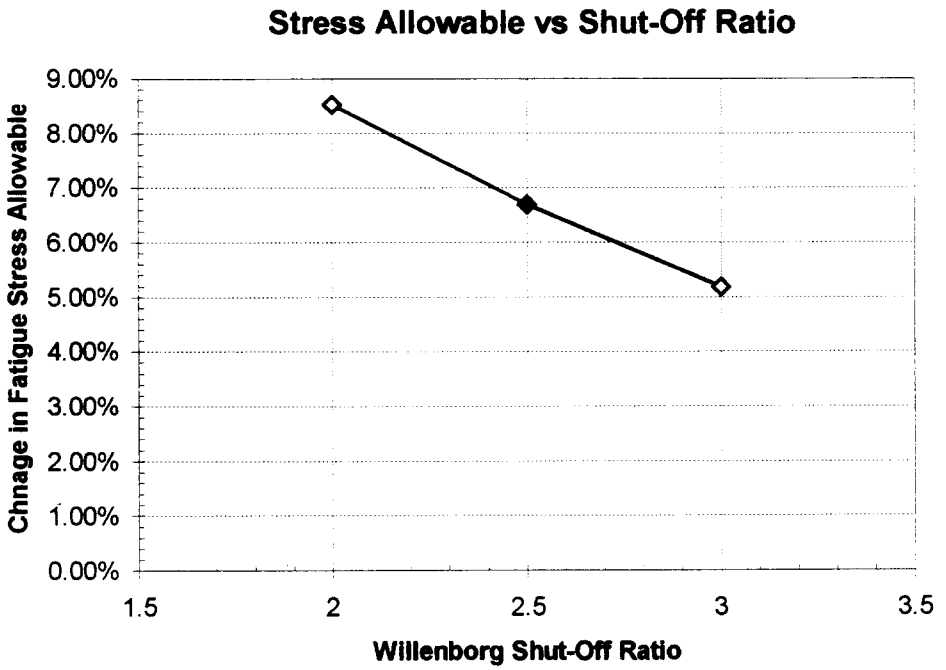

Figure 19: Effect of Retardation on Fatigue Stress Allowable

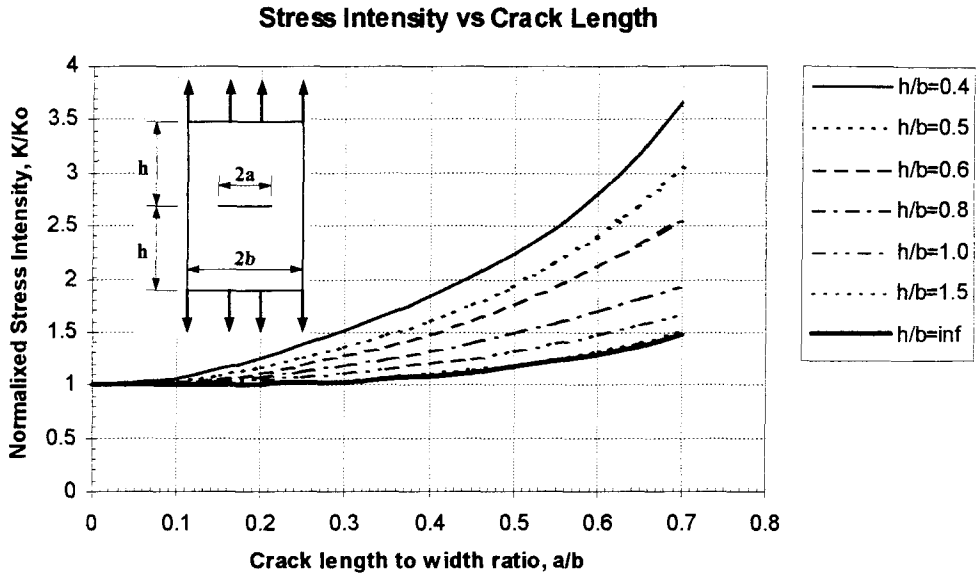

Figure 20: Stress Intensity for Finite Panels

intensity factor increases. As seen in Figure 20, the stress intensity increases as the ratio of length-to-width decreases. Theoretically, the finite panel solution must approach the infinite plate solution as the crack size decreases. Because the majority of a crack's life is spent at the smaller crack sizes, the effect of finite length and width should be somewhat diminished.

The effects of length and width will be examined independently. First, the length will be assumed to be infinite and the width will be varied. Then, the width will be held constant as the length-to-width ratio is varied. The stress intensity solutions in the MODGRO program account for finite width but not finite length. Therefore, the published [12] stress intensity data for finite plates (Figure 20) was used to create a $\beta_{correction}$ table to generate the appropriate stress intensities for a finite panel.

Width. The panel width was varied from 15.24 cm (6.0 in) to 121.92 cm (48.0 in). In Figure 21, the change in the fatigue stress allowable from the infinite plate

solution is plotted versus plate width. Even for very small panel widths the fatigue stress allowable did not change more than 3%. The actual panel (Figure 15) width of 30.48 cm (12.0 in), resulted in less than 1% change in the fatigue stress allowable.

Length. Similar results were obtained when the width was fixed at 30.48 cm (12.0 in) and the length-to-width ratio was varied from 0.4 to infinity. As seen in Figure 22, the maximum change in fatigue stress allowable was less than 2.5% for the F-16 wing panel near the wing root (Figure 15). The actual panel dimensions of 58.42 cm

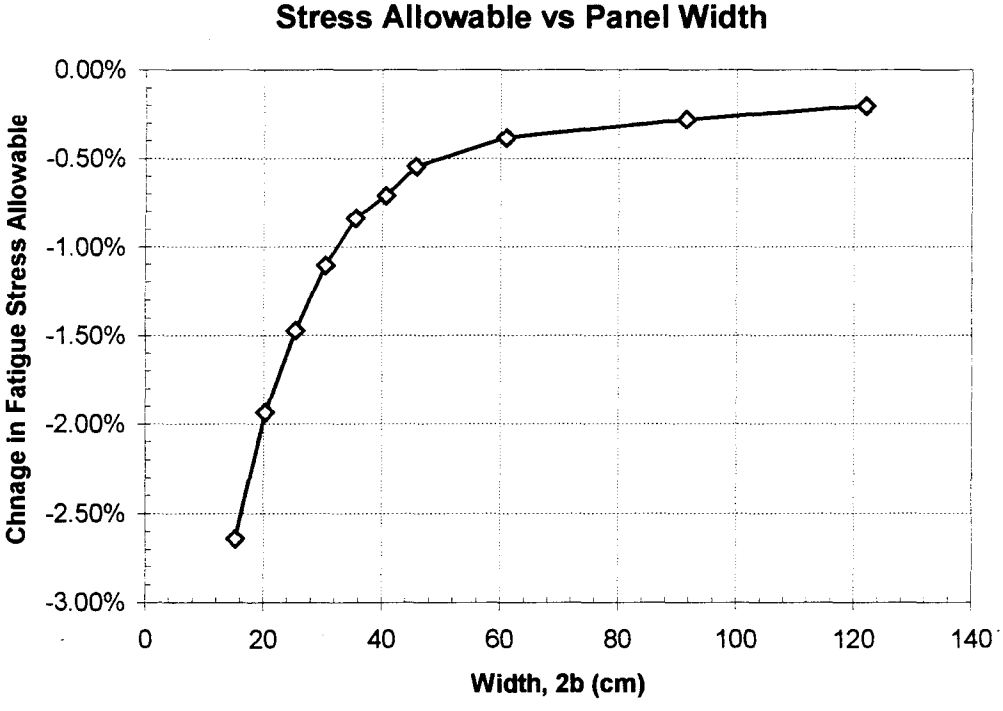

Figure 21: Change in Fatigue Stress Allowable vs. Panel Width

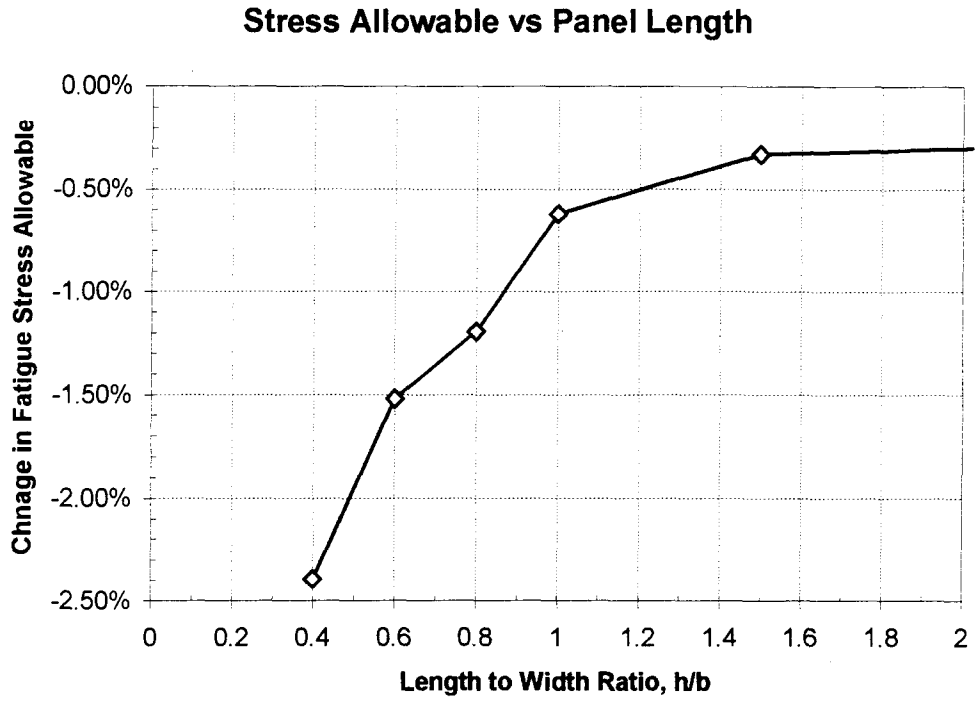

Figure 22: Change in Fatigue Stress Allowable vs. Panel Length

(23.0 in) by 30.48 cm (12.0 in) changes the fatigue stress allowable by about 2%.

Stiffened Panels. Aircraft wing panels are rarely simple sheets of metal as assumed in the previous analyses. Typically, the wing panel is constructed of numerous stringers riveted to a thin sheet (or skin). However, the global finite element model intentionally does not often include these structural details. Instead, the cross-sectional area of the stringers are often "smeared" across the finite elements and the rivets are usually ignored completely. In other words, the thickness of the finite elements in the wing panels are adjusted to produce a global behavior equal to the skin-stringer combination. This global structural modeling technique is ideal for calculating stress intensities in stiffened panels.

In Poe's method, the overall panel stress (stress applied to the skin-stringer combination) is used to establish the independent skin and rivet loadings in the stiffened panel. Therefore, stresses from "smeared" finite elements in a global aircraft model are exactly what are required for calculating stress intensities in a stiffened panel.

The stress intensity solutions for stiffened panels depend on three parameters: stiffener spacing, rivet spacing, and stiffness ratio (ratio of the stiffener and skin stiffnesses). The stiffness ratio is calculated by:

$$s = \frac{E_2 A}{E_1 bt} \qquad (7)$$

where s is the stiffness ratio, E_1 is Young's Modulus of the skin, E_2 is Young's Modulus of the stiffener, t is the skin thickness, b is the distance between stiffeners, and A is the

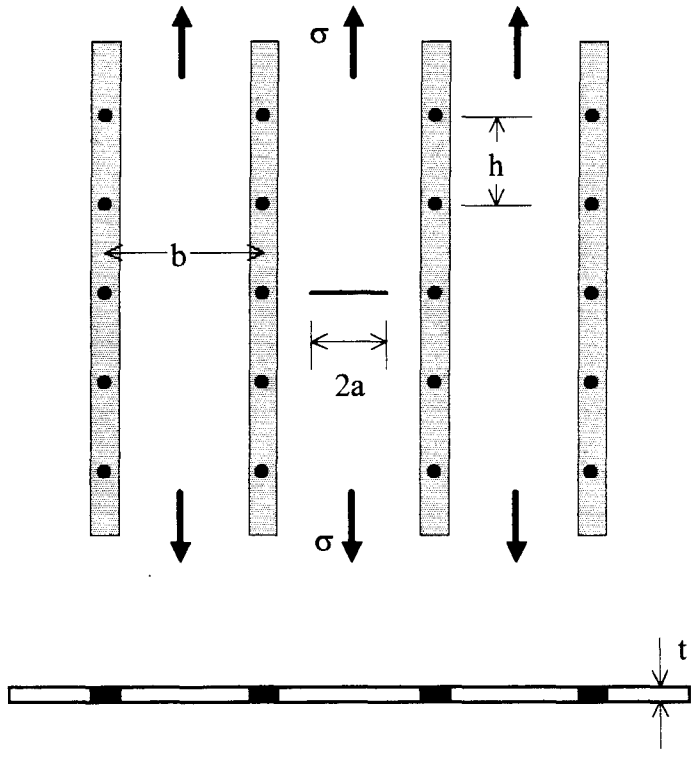

Figure 23: Stiffened Plate Geometry

cross-sectional area of the stiffeners (see Figure 23). If the skin and stiffeners are made of the same material (i.e. same Young's Modulus) then the stiffness ratio becomes the ratio of stiffener and skin areas.

The stress intensity as a function of crack length is graphically presented in Ref [12] for varying values of stiffener spacing, rivet-to-stiffener spacing ratio, and stiffness ratio. The stress intensities are normalized by the infinite plate solution (K_o) and plotted as a function of crack length (see Figure 24). The stress intensity "dips" as the crack approaches the stiffeners. These data were used as $\beta_{correction}$ tables in the MODGRO program to calculate the crack propagation in a stiffened plate.

A baseline condition was established and each of the parameters were varied independently about the baseline. The baseline consisted of a 15.24 cm (6.0 in) stiffener

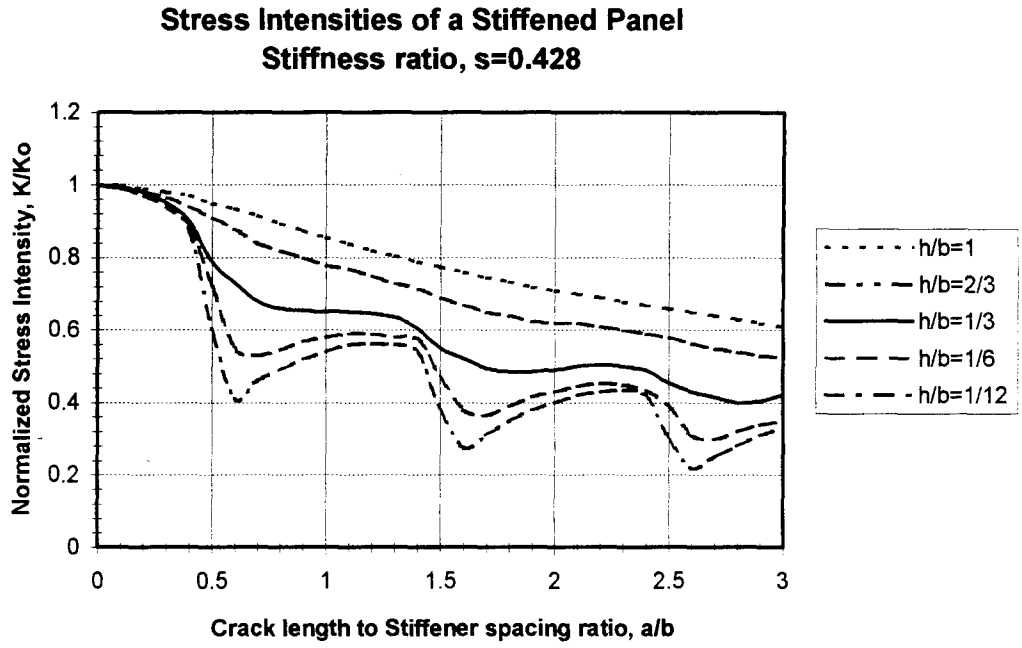

Figure 24: Example Stress Intensity Solution for Stiffened Panels

spacing, a rivet-to-stiffener spacing ratio of 1/3, and a stiffness ratio of 0.428 . In this manner, the effect of each parameter of the stiffened panel could be individually investigated.

Rivet Spacing. In Figure 25, the rivet-to-stiffener spacing ratio was varied from 1 to 1/12 while the stiffener spacing and stiffness ratio were held constant at the baseline values. The fatigue stress allowable was normalized by the non-stiffened, infinite plate result. As the number of rivets between stiffeners increases, more of the stress in the crack vicinity can be transferred to the stiffeners through the rivets. Therefore, the increase in fatigue stress allowable as the rivet-to-stiffener spacing ratio decreases was expected.

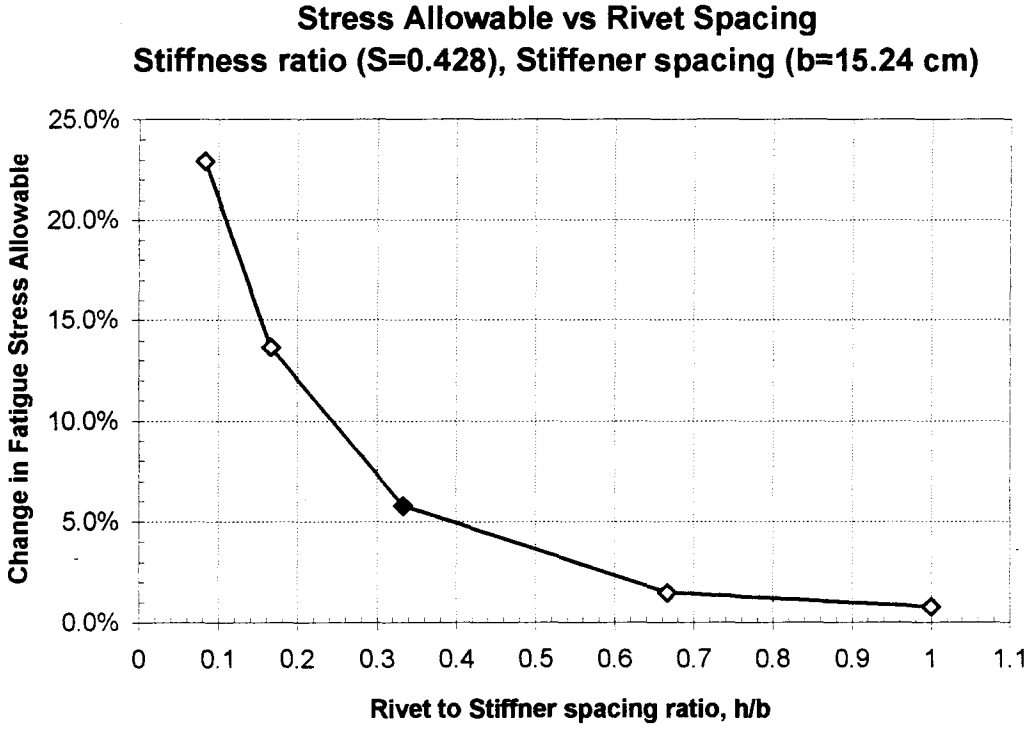

Figure 25: Effect of Rivet Spacing on Fatigue Stress Allowable

Figure 25 illustrates that the sensitivity of the fatigue stress allowable to the rivet spacing is significant. For example, a design change from a 5.08 cm (2.0 in) rivet spacing to a 2.54 cm (1.0 in) rivet spacing would increase the fatigue stress allowable by 7.4% . This could produce a significant weight savings in an aircraft design.

The stiffened panel stress intensities used above are based on Poe's analysis method which assumes that the rivets are rigid. Swift demonstrated that treating the rivet as rigid results in over-estimation of the stress intensity factor for small cracks and an under-estimation as the crack approaches the stringers. Since the majority of a crack's life is spent at small crack sizes, Poe's method should produce a conservative result.

Stiffness Ratio. The stiffness ratio was varied from 0 (no stiffeners) to infinity (no skin) while the other parameters were held constant. In reality, it is impossible to have a skin with zero thickness in a stiffened panel; however, it is theoretically possible because the stress intensity is not a function of panel thickness for a through-crack.

In Figure 26, the stiffness ratio is plotted versus the change of the fatigue stress allowable from the non-stiffened panel. As expected, the fatigue allowable increases as the material in the stiffened panel is shifted from the skin to the stiffeners. The limiting condition of an infinite stiffness ratio resulted in a 31.7% increase (not shown in Figure 25) in the fatigue stress allowable. Although stiffness ratios approaching infinity are not realistic for aircraft design, the data demonstrates that the fatigue stress allowable can be significantly increased even for much smaller ratios of stiffness (s=0.428) .

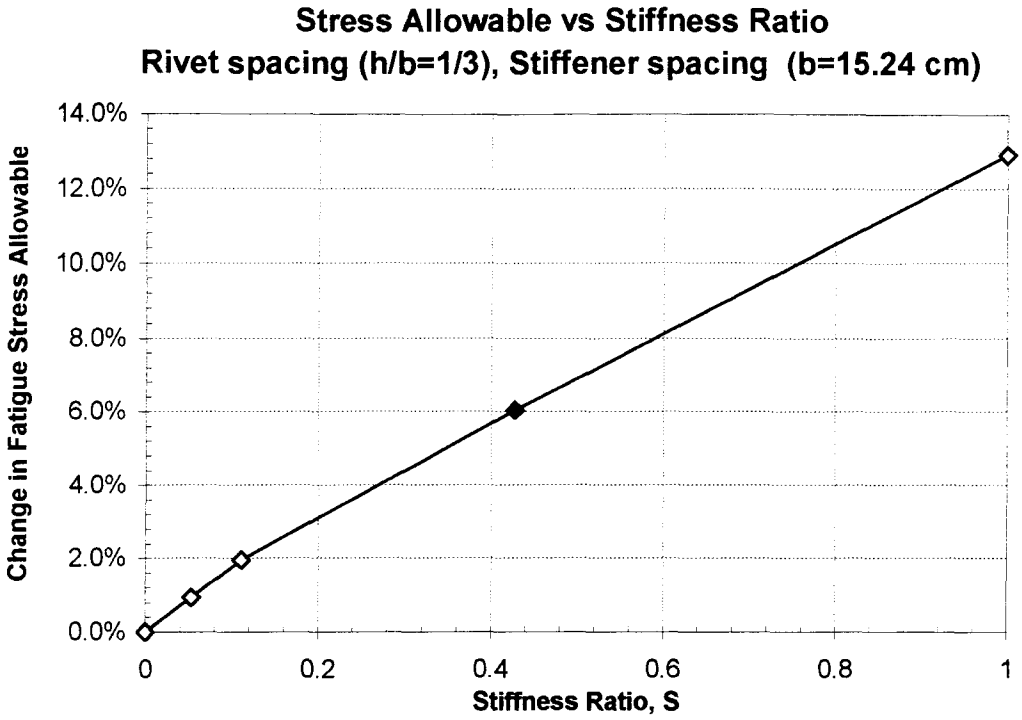

Figure 26: Effect of Stiffness Ratio of Fatigue Stress Allowable

Stiffener Spacing. Holding the rivet spacing and stiffness ratio equal to the baseline condition, the stiffener spacing was varied from 10.16 cm (4.0 in) to 25.4 cm (10.0 in). However, since the stiffness ratio is being held constant, the area of each stiffener must decrease proportionally as the stiffener spacing increases. The results illustrated in Figure 27 clearly show that the fatigue stress allowable increases when stiffeners are added to the wing panel. However, the results also indicate that the sensitivity of the fatigue stress allowable to stiffener spacing does not become significant until the stiffener spacing gets rather small (less than 15.24 cm).

These results would change for a less severe stress environment, such as the design usage of a transport aircraft. Transport aircraft are typically designed for a higher number of flight hours, but with much less severe stress levels. Therefore, the crack

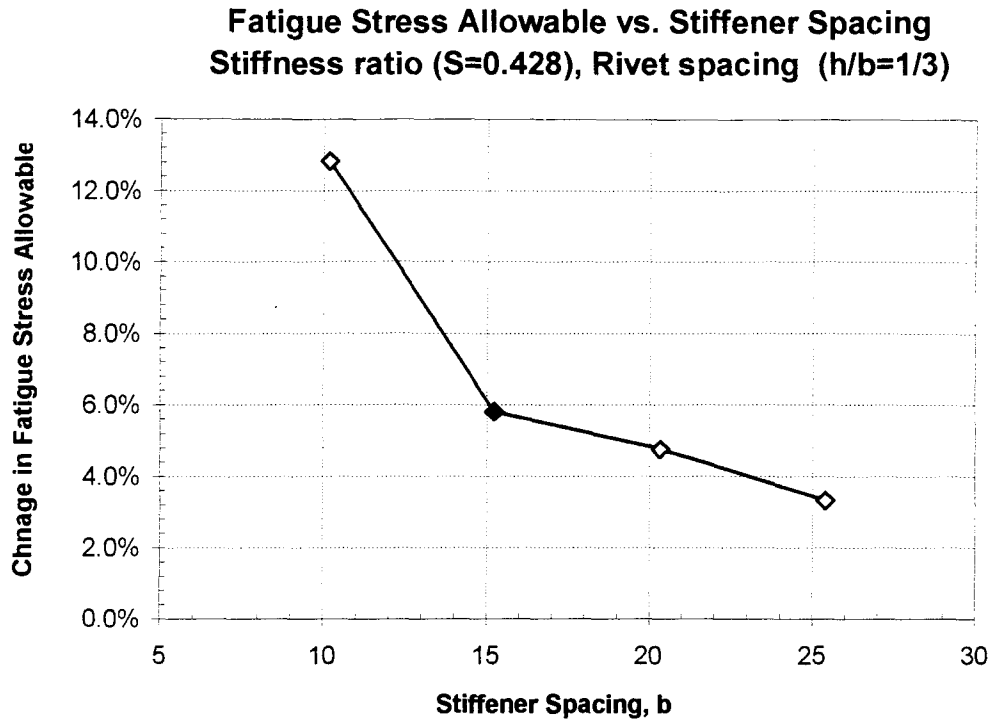

Figure 27: Effect of Stiffener Spacing on Fatigue Stress Allowable

would propagate at a slower rate over a longer distance than for a fighter aircraft. Since the stress intensity becomes progressively lower as the crack extends toward the stiffeners (see Figure 24), a long and slowly progressing crack would be more effected by the stiffeners.

Variation of Stress over the Wing

Panel Location on Wing. If an aircraft wing was a true cantilevered beam with a uniform bending load, then the location of the panel on the wing would have little effect on the normalized stress history. However, the stresses in an aircraft wing can be much more complex due to the wing's structural design, aerodynamic loading, control surface loading, weapon carriage loads, and other factors.

Although a sub-sonic transport aircraft may support wing stresses comparable to a cantilevered beam, the fighter aircraft modeled in the demonstration case is far from simple. Therefore, the normalized stress history for each panel in the demonstration wing would be expected to vary. This variation in panel stress histories is neglected in most current aircraft damage tolerant design simply because analysis of every panel would be too cumbersome. However, one of the advantages of the integrated, finite element based methodology presented in this thesis is the ability to easily extend the damage tolerance analysis to multiple panels.

A damage tolerance analysis was conducted on every wing panel in the demonstration case except for the hardpoint areas. Each panel was modeled as an infinite plate with a 0.635 cm (0.25 in) through-crack. Therefore, the only difference between each analysis was the difference in panel stress histories. The finite element nearest the panel's center was selected as the master element. Figure 28 illustrates the variation in fatigue stress allowables over the wing. The percentage change in fatigue stress allowable from the average allowable is indicated for each wing panel. The fatigue allowable varied approximately ±15% from the average across the wing. This amount of change in fatigue stress allowable cannot be ignored.

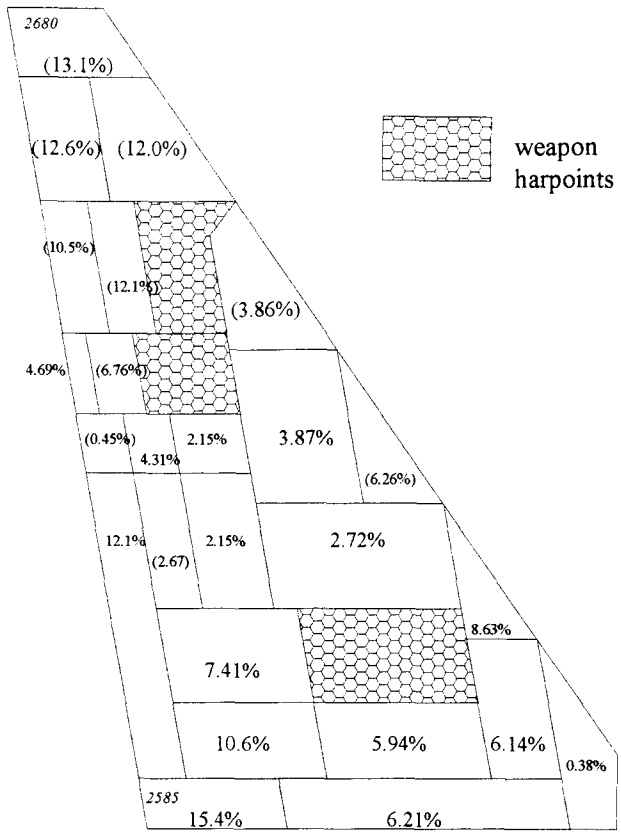

Figure 28: Variation of Fatigue Stress Allowable
(from the average) over the Wing

The other observation that should be made from Figure 28 is that the fatigue allowables tend to be higher near the wing root. The maximum fatigue stress allowable occurred at the trailing edge of the wing root and the minimum occurred at the wing tip. This result appears to contradict the traditional damage tolerance analysis which examines only the critical panels at the wing root area. However, remember that only the stress distribution of the wing is being allowed to vary and all of the panels are treated as infinite plates with a through-crack regardless of their actual dimensions and thicknesses. To obtain true results for fatigue stress allowables, all of the panel features must be modeled.

The stress exceedance distribution for the panels with the maximum and the minimum fatigue stress allowables are plotted in Figure 29. The panel with the lowest fatigue stress allowable is subjected to a more severe stress history containing many more stress occurrences between 90% and 100% of the panel's maximum stress. This is due to high stresses at the wing tip in the 5.86g unsymmetric maneuver (Load Case 107 in Table 3).

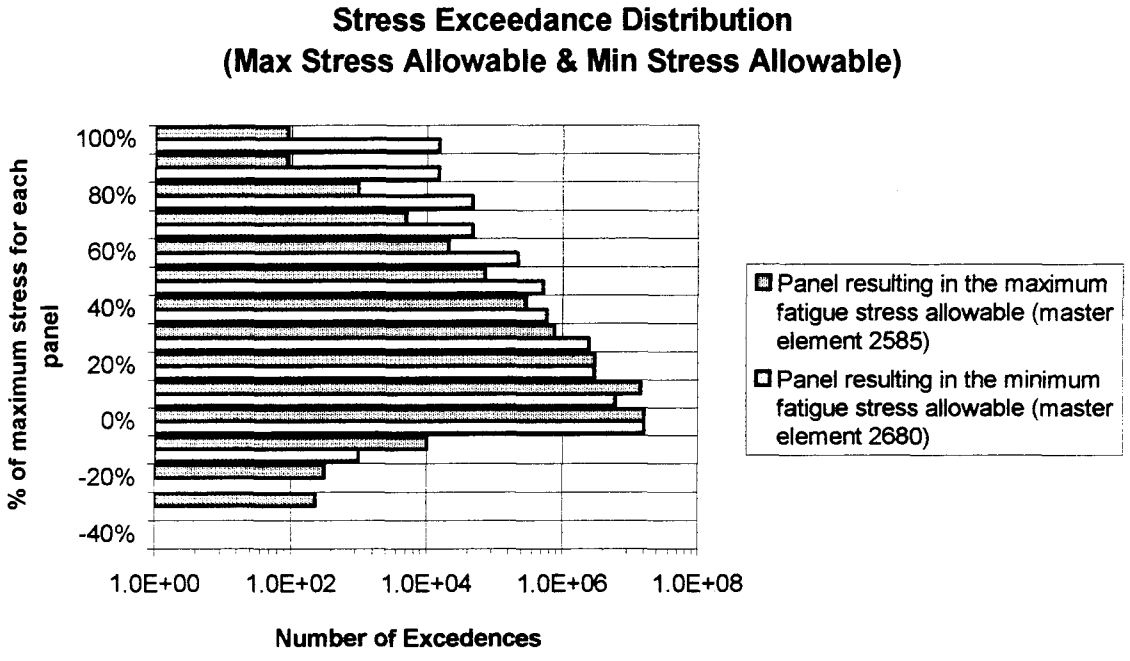

Figure 29: Difference in Exceedance Distribution for Panels with Max & Min Fatigue Stress Allowables

Panel Master Element. The maximum principal stresses used in the fatigue analysis of a panel are based on the master element designated by the user. For the above analysis the element nearest the center of the panel was selected as the master element, but what if a different master element was used? Three panels were selected to

investigate the sensitivity of the fatigue stress allowable to the master element: one near the wing root, one mid-wing between the weapon hardpoints, and one outboard of the weapon hardpoint (see Figure 30).

A damage tolerance analysis was performed using each finite element in the panels as the master element. The variation in fatigue stress allowable from the average allowable for each panel is shown in Figure 31, Figure 32, and Figure 33. Although the wing root panel and outboard wing panel displayed little sensitivity (less than 2.5%) to the choice of master element, the fatigue stress allowable for the mid-wing panel varied by as much a 6.5%. These results demonstrate that the selection of the master element for the panel can make a difference in some situations. Therefore, in areas of the wing

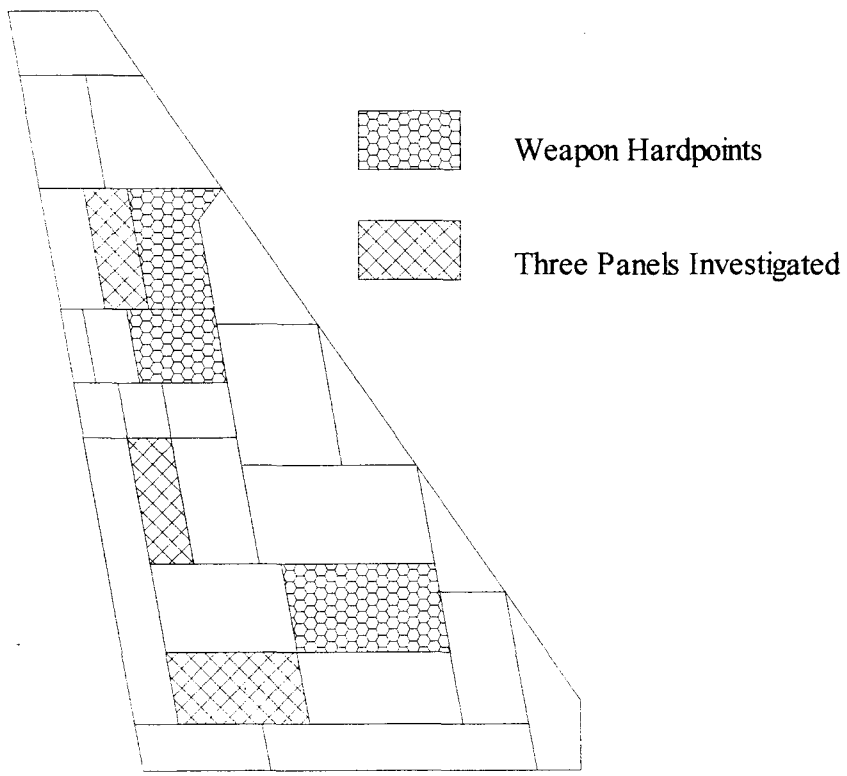

Figure 30: Three Wing Panels Investigated for Effect of Different Master Element

Figure 31: Variation in Fatigue Stress Allowable for Different Master Elements (Wing root panel)

with high stress gradients the master element should be selected carefully.

Optimization. The most important feature of ASTROS is its ability to optimize a structural design. In the case of wing panels, the panel thicknesses are adjusted to optimize the wing design. The objective of the optimization is to produce the lightest

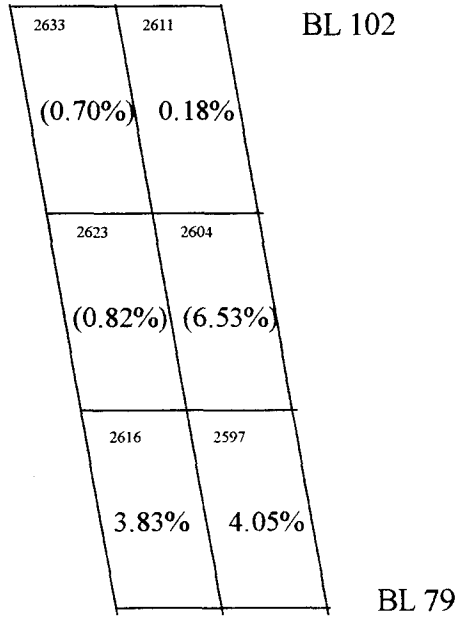

Figure 32: Variation in Fatigue Stress Allowable for Different Master Elements (Mid-wing panel)

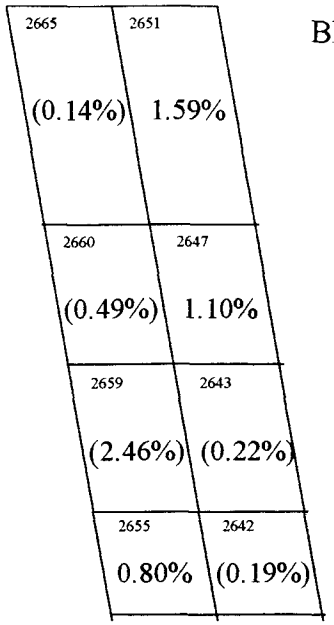

Figure 33: Variation in Fatigue Stress Allowable for Different Master Elements (Outboard wing panel)

possible wing without exceeding any of the design allowables. Of course, one of the design allowables used in wing design is the fatigue stress allowable.

The fatigue stress allowable is used as a wing design criterion during the ASTROS optimization to change the wing panel thicknesses. However, what effect does changing the wing panel thicknesses have on the fatigue stress allowable? The panel thickness can effect the fatigue stress allowable in two direct ways. First, the panel thickness is a critical parameter in the calculation of stress intensity for surface cracks. Second, adjusting the panel thicknesses changes the load path through the wing and, therefore, affects the panel stress histories. The objective of the last two trade studies was to determine the sensitivity of the fatigue stress allowable to the changes in wing panel thickness during the optimization process.

Thickness. For all of the prior trade studies, panel thickness was not considered because a through-the-thickness crack was assumed. However, panel thickness does become an important variable in the stress intensity calculation for surface cracks. The slow-crack growth criteria set forth by the USAF specifies two different types of surface cracks: a semi-elliptical surface crack, and a corner crack at a hole. Figure 34 and Figure 35 illustrate the crack dimensions for the two surface cracks. The criteria does not specify a hole diameter for the corner crack so a reasonable rivet hole size of 0.508 cm (0.2 in) was assumed.

The ratio of panel thickness to minor axis (through-thickness direction) crack length was varied for the two crack types. The thickness to crack length ratio equal to one is identical to a through-crack solution. In Figure 36, the change in fatigue stress allowable from the through-crack solution is plotted for different thickness ratios. Clearly, the fatigue stress allowable demonstrates a significant amount of sensitivity to the panel thickness when the crack is a semi-elliptical surface crack.

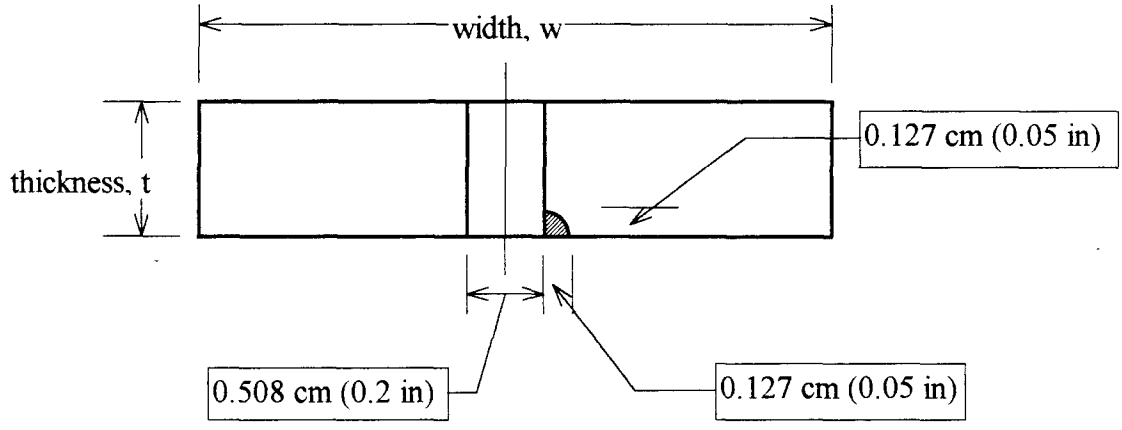

Figure 34: Corner Crack at Hole

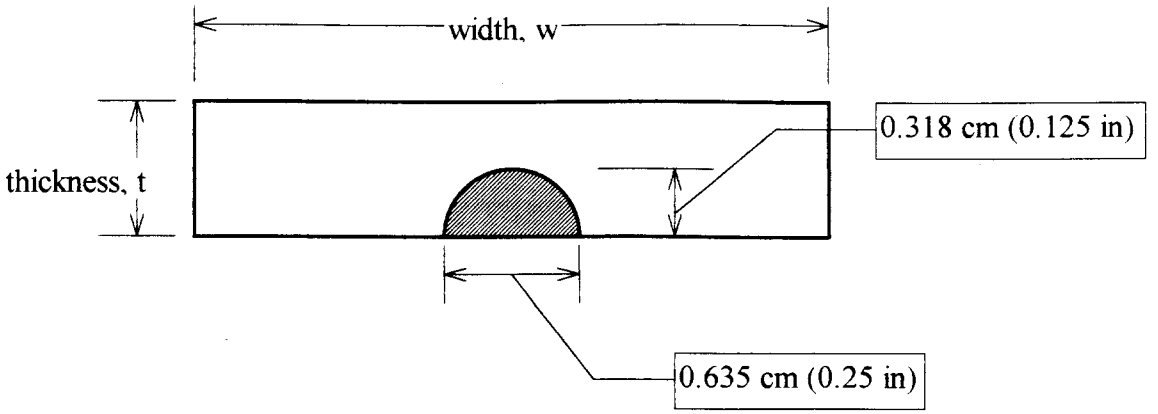

Figure 35: Semi-Elliptical Surface Crack

Variation of Stress. When a wing is optimized in ASTROS, all of the wing panels are often initialized to a constant thickness. During the optimization, the wing panel thicknesses are altered to produce resulting stresses close to, but not

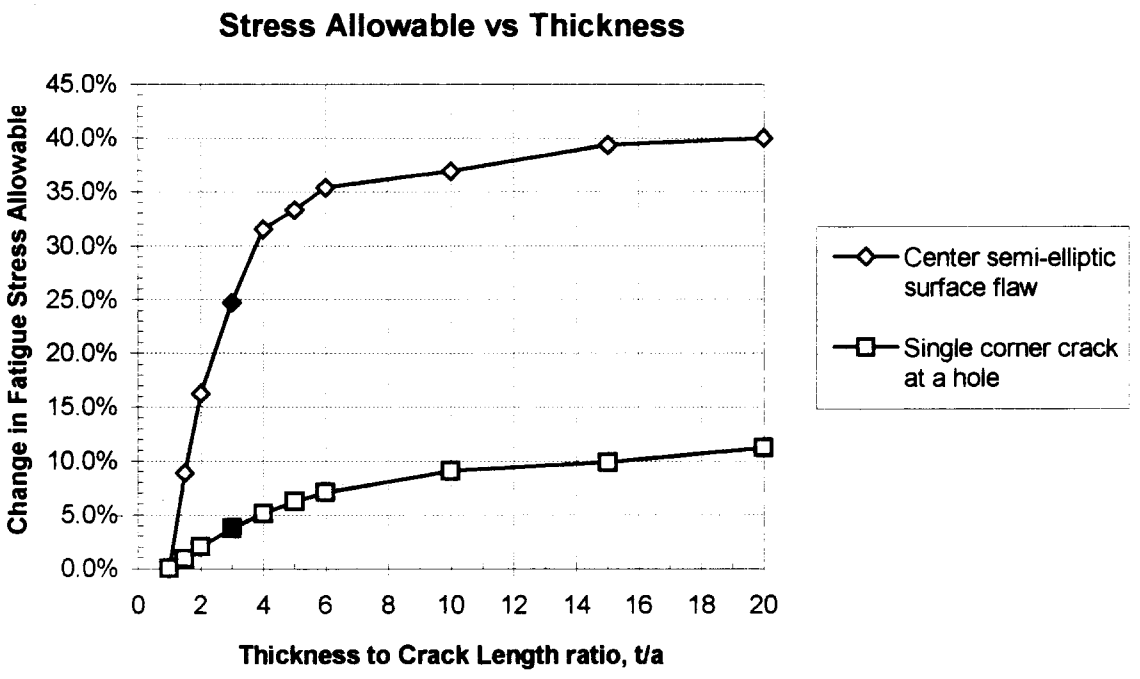

Figure 36: Effect of Panel Thickness on Fatigue Stress Allowable

exceeding, the design allowables. Clearly, the load paths throughout the wing are affected by the optimization process and, hence, the panel stress histories are changed as well.

The wing panel thicknesses in the demonstration model are based on the production F-16 design. Therefore, the thicknesses in the model represent a wing that has already been optimized to some extent. For comparison purposes, the model was modified so that all of the wing panel elements were 0.625 cm (0.25 in) in (smeared) thickness. The results of this modified model are similar to a wing before being optimized. The fatigue stress allowables for a through-crack were calculated for the constant thickness wing model and compared to the original demonstration model.

Figure 37 illustrates the change in the fatigue stress allowables from the constant thickness model to the "optimized" model. The majority of the fatigue stress allowables only changed ±2%; however, the fatigue stress allowable for one panel decreased by 14% for the optimized wing. Therefore, the fatigue stress allowable calculated prior to optimization is non-conservative. Ignoring the change in fatigue stress allowables due to optimization could lead to a reduced service life of the production aircraft. However, it is important to note that this change in fatigue stress allowable is due only to the change in stress distribution in the wing caused by the change in panel thickness and not to the panel thickness itself. The direct effect of panel thickness on the fatigue stress allowable (see Figure 36) is eliminated because a through-crack is assumed for all panels.

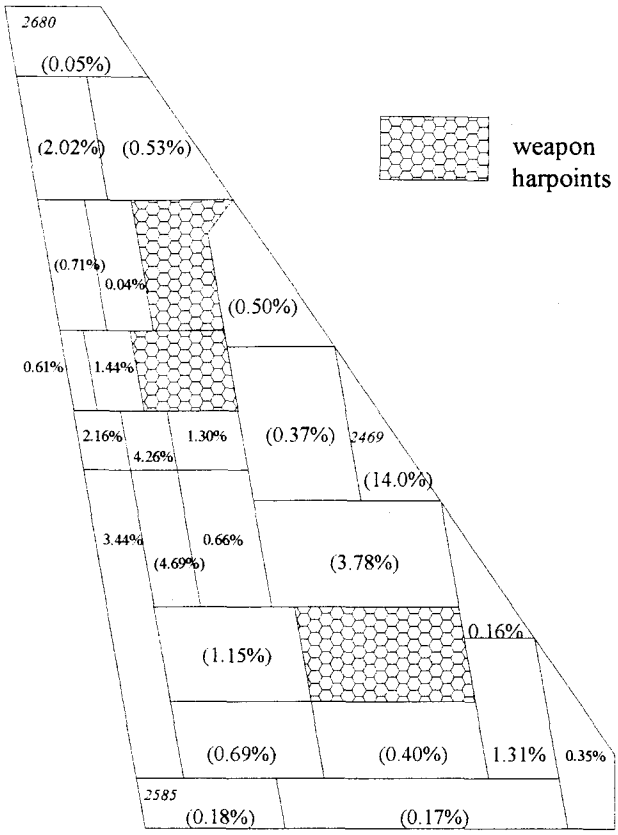

Figure 37: Change in Fatigue Stress Allowable due to "Optimization"

V. Recommendations

The results and discussion of the trade studies were presented in the previous chapter. However, further discussion of these results from the perspective of overall design practices is warranted. The discussion can be separated into three major categories: crack propagation prediction, local wing panel modeling, and optimization. For each category, the most important results from the trade study are discussed further, and then recommendations are made for future work in this area.

The first two topics are concerned with the analysis tools and modeling details required for a valid damage tolerance analysis of aircraft wing panels. However, the third subject is distinct because it focuses on the role damage tolerant design can play in multi-disciplinary optimization (MDO) of aircraft.

Crack Propagation Prediction

Material Properties. The results from the trade study clearly demonstrate that the fatigue properties (da/dN vs. K) of the material have a major impact on the fatigue stress allowable. In contrast, the material's fracture toughness had little effect on the fatigue stress allowable. Although the effect of fracture toughness will vary depending on the particular situation, these data support that the fatigue data deserves much more

emphasis than the fracture toughness. These results re-emphasize the need for coupon testing when the material selection is completed.

In this study, the Walker equation was used to represent the *da/dN* vs. *K* material data; however, more complex equations have been developed that may better represent the data. In addition, the MODGRO program allows tabulated material test data to be used instead of a curve-fit equation. Due to the sensitivity of the damage tolerance analysis to the fatigue properties, careful thought should be put into the method used to represent the available *da/dN* vs. *K* data.

Mixed-Mode Stress Intensity. As discussed earlier, the issue of fatigue for mixed mode stresses was resolved by using the maximum principal stress as an equivalent stress in pure mode I cracking . Although this method has been validated for constant amplitude fatigue, very little testing has been performed to characterize the effects of varying the direction of principal stresses. Therefore, wing designs dominated by bending stresses (usually wings with high aspect ratios) can be analyzed using the maximum principal stress assumption with a relatively high degree of confidence. However, for wing designs like the F-16 demonstration case, the fatigue stress allowables are less reliable due to the large variations in maximum principal stress direction in the wing (see Table 4).

Additional research in the area of mixed-mode fatigue is required to validate or refine the method applied in this study. However, in the meantime, this remains the only approach for handling mixed mode fatigue without extensive computational analysis.

Multi-Phase Crack Propagation. All of the analyses performed in this study were for an initial crack at the center of the panel. Rooke and Cartwright's compendium of stress intensity factors [12] indicates that the stress intensity decreases for an eccentrically located crack; therefore, a center crack is usually a conservative assumption. However, if the crack is close to the edge it can propagate all of the way to the panel edge without causing panel failure. Therefore, the crack propagation must transition to an edge crack and continue in the other direction until catastrophic failure. The transitioning of a crack propagation from one crack type to another can be referred to as multi-phase crack propagation.

Figure 38 illustrates different phases of crack propagation for a corner crack at a hole near the panel edge. The crack starts at the primary crack site and propagates in Phase 1a until it transitions to a though-crack in Phase 1b. After N number of cycles, the crack reaches the edge of the panel. Simultaneously, the secondary crack has also been propagating. However, the interaction between two cracks is extremely difficult to predict. Therefore, current design guidelines specify that the secondary crack should be propagated for the same N cycles as if the primary crack did not exist. This is sometimes referred to as *cumulative damage* and is labeled as Phase 2a & 2b in Figure 38. In this example, it was assumed that the crack transitions to a through-crack during the cumulative damage phase. After the cumulative damage is calculated, the crack resumes propagation at N cycles in Phase 3 until failure.

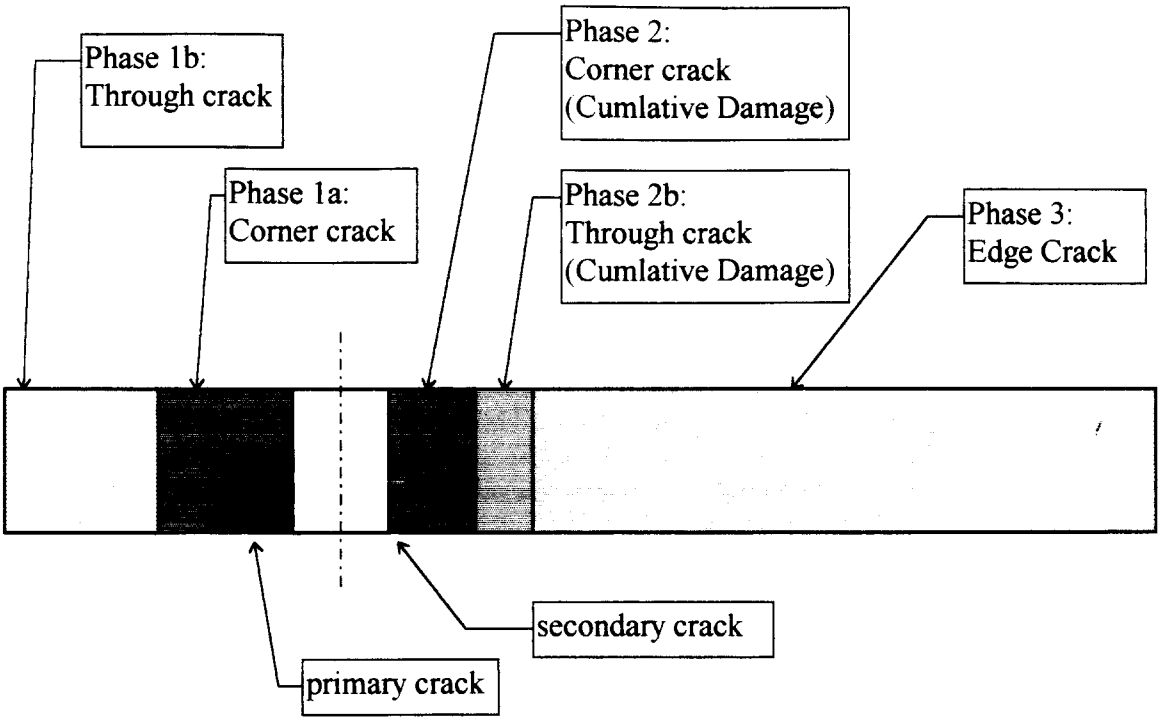

Figure 38: Multi-Phase Crack Propagation

The MODGRO program currently can handle the transition from a surface-crack to a through-crack. Although each phase of the above multi-phase problem could be modeled in MODGRO, the program cannot automatically perform the necessary transitions. The multi-phase crack propagation is a difficult problem to model, but it is a real-life situation that occurs in aircraft wing panels. Therefore, the capability to perform multi-phase crack propagation should be considered for any production level application of this methodology.

Local Wing Panel Modeling

Finite Length and Width. The effect of finite length and width on the fatigue stress allowable for a center crack was shown to be relatively small compared to the other parameters (less than 2.5%). In fact, ignoring the finite width and length correction would be acceptable in for many panel geometries. Therefore, using approximate measurements of length and width should have very little adverse effects.

Stiffened Panels. The results in Chapter IV clearly demonstrate that the detailed (local) design of a stiffened panel has a significant effect on the fatigue stress allowable. The fatigue stress allowables for stiffened panels were calculated using tabulated stress intensity data for specific values of the three design parameters: stiffener spacing, rivet spacing, and stiffness ratio. Although this was sufficient for the trade studies, it does not provide adequate flexibility to model all possible variations of stiffened panels. Therefore, it is recommend that Poe's displacement-matching technique be implemented in the crack growth prediction code. In addition, a stiffened panel routine could be further enhanced by including the effects of rivet flexibility as described by Swift.

Although Poe's displacement-matching technique is less computationally demanding than detailed finite element analysis, it still involves the simultaneous solution of a system of linear equations. If the system of equations had to be solved for every crack length in the stress history, the computational requirements would become unreasonable. Therefore, it is recommended that Poe's method be implemented by calculating a $\beta_{correction}$ table for the specific stiffened panel design prior to the crack

propagation. This procedure would add the flexibility of handling varied stiffened panel designs without a disproportionate increase in computational requirements. In addition, the user could specify a stiffened panel by only three or four parameters instead of manually producing a $\beta_{correction}$ table for every panel.

Wing Spars. Unlike the wing panel stringers, the spars in the wing are modeled separately in most global aircraft models. The finite element analysis distributes the wing loading between the wing panels and wing spars. Therefore, the method used to calculate the effect of panel stiffeners on the crack stress intensity cannot be applied to the panel/spar interface. In the case of widely spaced wing spars and center cracks, the effect of the wing spars on the stress intensity should be negligible due to Saint-Venant's Principle. However, in some aircraft the wing spars are very closely spaced (the F-16 wing spars are only 20.32 cm (8.0 in) apart). In addition, the crack may be located at one of the rivets attaching the panel to the spar instead of at the center of the panel. In these situations, the effect of the wing spars on the fatigue stress allowable cannot be arbitrarily ignored. Therefore, additional research is required to develop a means of calculating the effect of wing spars on the stress intensity using the data available in the global finite element model.

Optimization

Current Recommendation. Using ASTROS, the global wing design can be optimized. The design changes in the wing during the optimization can effect the fatigue

stress allowables in two ways: through the panel thickness and the stress distribution in the wing (panel stress history). The trade studies clearly showed the change in panel thickness could cause a significant change in the fatigue stress allowable for certain surface crack types. The fatigue stress allowable was also effected by the change in panel stress histories, but not nearly as much.

Although the changes in fatigue stress allowables due to optimization are large enough that they shouldn't be ignored, they are not significant enough to justify the computational expense of updating the fatigue stress allowable after each iteration of the optimization loop. Therefore, it is recommended that the damage tolerance analysis not be included inside the optimization loop. However, the fatigue stress allowables should be updated at least once during the optimization process. This can be accomplished by the following process:

1. Estimate the fatigue stress allowables based on the non-optimized design.
2. Perform the optimization.
3. Update the fatigue stress allowables based on the optimized design.
4. Resume the optimization until convergence.

Figure 39: Recommended Method of Updating the Fatigue Stress Allowables for Optimized Wing Design

Stiffened Panel Algorithm. As discussed above, changes in the design parameters of stiffened panels caused significant changes in the fatigue stress allowables. However, the global finite element model only considers the stiffeners in the panel by

"smearing" the stiffener area across the panel elements. After the global design is completed, the smeared panel thickness is used to perform the local design of each panel. During the local design, the stiffener spacing, stiffener area, and rivet spacing are specified.

Suppose that the design process used to specify the local stiffened panel design could be captured in an algorithm. The algorithm could use the smeared panel thicknesses to select between several typical stiffened panel designs used by the particular manufacturer. With this algorithm, the local stiffened panel design could be estimated from the global design and used in the fatigue stress allowable calculation. This algorithm would not replace a more rigorous local panel design process, but merely estimate the stiffened panel design for the purposes of the damage tolerance analysis. Ideally, this would occur in step 3 of the outlined optimization process. Implementation of this procedure could reduce the number of design iterations between the local and global design.

Parametric Finite Element Modeling. Currently, Wright Laboratories is conducting research in the area of Parametric Aerospace Design [28] . With parametric modeling "detailed geometric dimensions are defined relative to more coarse geometric features. If fundamental parameters are changed, then all subsequent dimensions are updated [28] ." If parametric finite element modeling was implemented, major wing design features such as wing sweep and aspect ratio could be optimized. Based on the results for optimizing panel thickness alone, parametric optimization of the wing could have dramatic effects on the wing panel fatigue stress allowables. If parametric

modeling is implemented in future wing optimization, damage tolerance analysis procedures similar to the one developed in this thesis would be essential.

Design Usage

System Resources. The USAGE program uses mission segment load-exceedance spectra to ultimately define the load history of the aircraft in terms of ASTROS load cases. This procedure is consistent with current design usage development guidelines and design practices. The program provides a powerful tool capable of modeling very complex and detailed aircraft design usage. However, the current programming technique maintains all of the design usage data in the system's dynamic memory. This could become a limiting factor for some systems. Therefore, it is recommended that the design usage program be rewritten to take advantage of the CADDB relational database features used in ASTROS. This would provide a virtually limitless modeling capability.

Application of Probability. The load-exceedance spectra used to model the aircraft usage is a discrete probability distribution produced from actual aircraft measurements. The measurement data could also be modeled by an appropriate continuous probability distribution function. There are commercially available software tools that are specifically designed to fit experimental data to probability distribution functions. Therefore, a load-exceedance spectrum could be specified by only several parameters. Since a continuous function does not have discrete load levels like a load-

exceedance spectrum, a distribution function range would be specified as a specific ASTROS load case.

The ASIP flight measurement program records many other variables besides the vertical load factor. Therefore, a bivariate or even multivariate probability distribution could be developed from the data. For example, the aircraft roll rate could be used to establish the bivariate probability of unsymmetric maneuvers and vertical load factor.

The use of probability distribution could be extended beyond the load-exceedance spectra to the distribution of missions throughout the life of the aircraft. Although the load cycles within a mission segment are randomly sequenced, the mission order currently must be specified by the user. Using probability distributions, the order of missions in the life of an aircraft could be randomly sequenced.

The return on investment for applying more advanced probability theory to the development of the aircraft design usage is debatable. In the end, the decision of whether or not to utilize continuous probability distributions should be left to the preferences of the aircraft manufacturer.

Interfacing with ASTROS

Panel Geometry. The use of the buckling constraint bulk data card (DCONBK) to obtain panel length and width was very advantageous for this study. However, given the relatively low importance the panel dimensions played in the fatigue stress allowable,

it seems unnecessary to burden the user with the task of specify the length and width of the panels. It would be more convenient for the user to specify a list of finite elements in the wing panel from which the program could automatically calculate the average panel dimensions from the elements.

Updating Fatigue Stress Allowables. The number of iterations required to converge to the fatigue stress allowable depends on how good the initial guess is. If the user could provide a better estimate of the fatigue stress allowable, then the computation time could be significantly reduced. In addition, the results of the damage tolerance analysis could be used to automatically update the fatigue stress allowable in the ASTROS database (step 3 of Figure 39). This would eliminate the need to manually update the fatigue stress allowable before the optimization process is started or resumed. Each time the damage tolerance analysis is repeated, the most recent fatigue allowable would be used as the initial guess for the iteration process.

ASTROS Panel Bulk Data Card. If a production software code is developed to link a damage tolerance analysis with ASTROS, then a new ASTROS bulk data card should be created to input the necessary panel information. The following is one possible format for the panel design constraint data card:

1	2	3	4	5	6	7	8	9	10
DCONPAN	PANID	FALLOW	EID0	EID1	EID2	EID3	EID4	EID5	CONT

Field	Contents
PANID	Panel Identification number
FALLOW	Fatigue stress allowable used as the design allowable for the panel's maximum principal stress. (This allowable will be used as the initial guess for any

	subsequent damage tolerance analysis and will be updated after each analysis)
EID0	Element Identification number for the master element. (If left blank, the largest maximum principal stress from the elements listed in EIDn will be used in the fatigue stress allowable calculations).
EIDn	List of element identification numbers for the elements that define the wing panel.

Using this bulk data format, a panel can be uniquely specified by the panel identification number (PANID). Therefore, the input to the damage tolerance analysis program would specify the wing panel in the ASTROS model through the PANID. During the optimization, the current fatigue stress allowable (FALLOW) would be used as the design allowable for the maximum principal stress in the panel elements. The user can specify a master element to control the panel stresses or, by default, the largest stress from the list of elements in the panel would be used. In addition, the average panel width and length would be calculated using the nodal coordinates of the elements in the panel.

Programming Recommendations

Convergence Routine. In general, the convergence routine used in this study performed adequately. However, in certain situations the program had difficulty with convergence. As discussed in Chapter 3, a least-squares curve fit of previous results is used to predicted the fatigue stress allowable in the next iteration. The difficulty in convergence occurred when a very small change in the fatigue stress allowable caused a

extremely large change in the number of cycles to failure. This situation arose several times when the stiffened panels were being analyzed. The "humps" and "dips" in the stress intensities near the stiffeners (see Figure 24) sometimes caused large overshoots in the fatigue stress allowable prediction. Although the iteration did not diverge, the rate of convergence was not acceptable. Therefore, it is recommended that a more robust routine be developed to increase the rate of convergence.

Program Structure. The program structure used in this study is illustrated in Figure 5. For the purpose of this study, the MODGRO program was selected to perform the crack growth propagation. However, the MODGRO program is a general application program not specifically designed for this purpose. Therefore, the interaction between the PANEL program and MODGRO was not very efficient. If this design methodology is to be implemented, the programs structure should be changed to tailor it to this particular application.

The USAGE program is a stand-alone program which requires no information from the ASTROS database or from the PANEL program. Since the load history developed by the USAGE program applies to all of the wing panels in the aircraft and is not effected by panel design changes, it should remain a separate program.

The three primary tasks of the PANEL program are: to read the user input, interface with the ASTROS database to obtain panel geometry and stresses, and iterate around the MODGRO crack growth analysis until convergence of the fatigue stress allowable. To make this methodology more efficient, the functions of the PANEL program and MODGRO program should be combined into a single program as shown in

Figure 40. The iteration and convergence of the fatigue stress allowable would be handled internal to the FATIGUE program. In addition, the fatigue stress allowable for each panel would be automatically updated in the ASTROS database. This program structure would increase the efficiency by eliminating the need to transfer information via data files. However, this does sacrifice the modularity of the program structure which would make it more difficult to substitute different crack growth prediction routines.

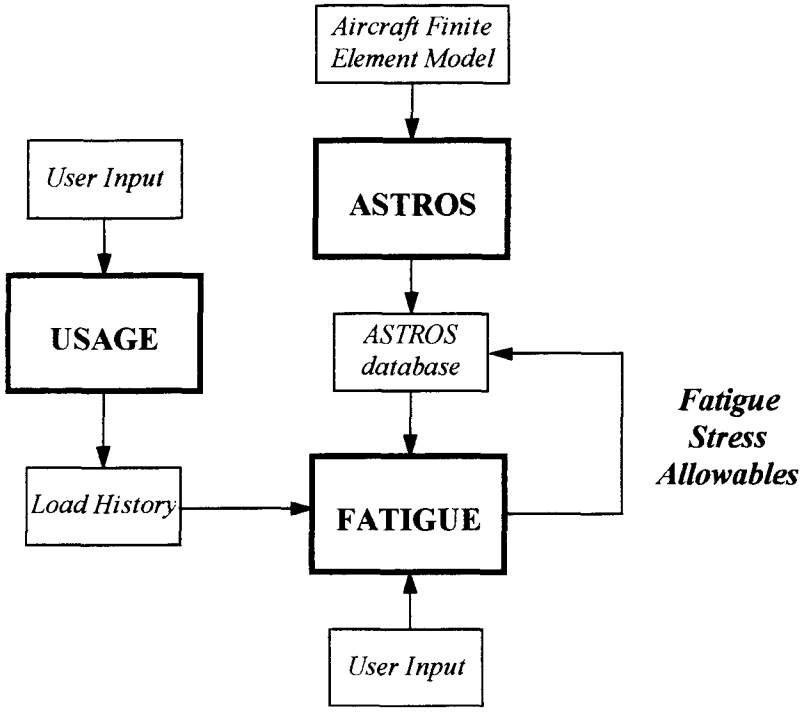

Figure 40: Recommended Program Structure

VI. Conclusions

A methodology for implementing fatigue design issues into the global design of aircraft in the ASTROS design environment was developed using current damage tolerance design guidelines and analysis techniques. The methodology represents a fusion of the ASTROS finite element capabilities with various independent procedures and analytical tools for fracture mechanics, fatigue analysis, and aircraft design usage.

Mixed-mode fatigue is one area that deserves future attention. Following published recommendations, the mixed-mode fatigue situation was handled by using the maximum principal stress as an "effective" stress in pure mode I fatigue. However, this procedure has not been adequately validated for components subjected to the complex stresses typical in real-life aircraft design. Additional experimental research is required before this procedure can be confidently applied to aircraft wings subjected to a high degree of mixed-mode fatigue.

The methodology was implemented into a software code to facilitate an investigation of the effect of different design variables on the aircraft design. The trade studies indicated that the sensitivity of the fatigue stress allowable to the panel design warrants the analysis of all wing panels instead of only the critical panels at the wing root. This could not only result in a decrease in unexpected fatigue problems, but also an increase in aircraft performance through a weight savings in less critical panels.

The panel design features that had the most significant effect on the fatigue stress allowables were: material fatigue properties, stiffened panel design, panel thickness, and panel location on the wing. Based on these results, other capabilities were recommended for implementation in the methodology, including: the effect of the wing spars on the fatigue analysis and the capability to automatically handle complex multi-phase crack scenarios.

Although the effect of optimization was not large enough to justify that the damage tolerance analysis be updated after each iteration in the optimization loop, it also could not be ignored. To avoid significant inaccuracies in the fatigue stress allowable (both conservative and non-conservative) the fatigue stress allowable must be updated at least once as the design approaches final convergence.

Damage tolerance has only been a part of aircraft design for a little more than two decades. In this time, many advances have been made in this field; however, damage tolerant design is still in its infancy. With the recent emphasis on multi-disciplinary optimization (MDO), damage tolerance is only one of many engineering disciplines that are being reexamined for integration into aircraft optimization. The ultimate goal is to develop an optimization procedure capable of increasing the safety and performance of modern aircraft while reducing the time and cost of development. It is hoped that the methodology presented in this thesis can act as a starting point for future developments and refinements in this area of research.

Appendix A: USAGE Program User's Guide

The USAGE program creates an aircraft's design usage load-history file defined in terms of ASTROS load cases. The program is executed by the following statement:

USAGE *input_filename*

Field	Contents
input_filename	Filename of the USAGE input file (.inp) NOTE: The (.inp) extension is not specified at the command line.

The load history file is written to a file with the same base name as the input file but with a (.dat) extension (i.e. *input_filename*.dat) . The input echo and results summary is written to the default system output. The input file consists of 80 column text lines called "bulk data entries," organized in "fields" of eight characters according to NASTRAN conventions. The bulk data entries which constitute the input file are described in the next section.

Input Format:

SPECTRUM -- This command is used to specify the spectrum load-exceedance (or load-occurrence) data.

1	2	3	4	5	6	7	8	9	10
SPECTRUM	SPECID	EX/OC	*** SPECTRUM DESCRIPTION TEXT ***						
NZ1	NUM1	NZ2	NUM2	NZ3	NUM3	NZ4	NUM4		CONT

Field	Contents
SPECID	Spectrum Identification number (integer)
EX/OC	Specifies whether the spectrum data is exceedance data or occurrence data (character)
NZn	Vertical load factor for load level n (real)
NUMn	The number of exceedances/occurrences in load level n per 1000 flight hours (integer)

SEGMENT1 -- This command is used to define the segment data when each load level has only one maneuver type. A segment definition consists of a spectrum (SPECID) and a maneuver description for each load level in the spectrum. The maneuver is defined in terms of an ASTROS solution (boundary condition and load case).

1	2	3	4	5	6	7	8	9	10
SEGMENT1	SID	SPECID	BID0	LOAD0	SCALE0	BID1	LOAD1	SCALE1	CONT
BID2	LOAD2	SCALE2							

Field	Contents
SID	Segment Identification number (integer)
SPECID	Spectrum Identification number (integer)
BIDn	ASTROS Boundary Identification number for load level n (n= 0 is for 1 g level flight condition) (integer)
LOADn	ASTROS Load Case Identification number for load level n (integer)
SCALEn	Scale factor for the stress for load level n (real)

SEGMENT2 -- This command is used to define the segment data when load levels have more than one maneuver type. A SEGMENT2 data card is required for each load level in the spectrum and a 1g level flight condition.

1	2	3	4	5	6	7	8	9	10
SEGMENT2	SID	SPECID	LEVEL	BID1	LOAD1	SCALE1	PERCENT1		CONT
BID2	LOAD2	SCALE2	PERCENT2						

Field	Contents
SID	Segment Identification number (integer)
SPECID	Spectrum Identification number (integer)
LEVEL	Load Level (LEVEL=0 for 1g level flight condition) (integer)
BIDn	ASTROS Boundary Identification number for maneuver n in this load level (integer)

LOADn	ASTROS Load Case Identification number for maneuver n in this load level (integer)
SCALEn	Scale factor for panel stresses for maneuver n in this load level (real)
PERCENTn	Percentage of the load occurrences in this load level that correspond to maneuver n (real)

MISSION -- A mission is defined as a sequence of mission segments. Each segment is specified by the Segment ID (SID) and a number of flight hours. The order of mission segments in the mission follows the order of the input card. However, the sequence of the load cycles within each mission segment is randomly ordered.

1	2	3	4	5	6	7	8	9	10
MISSION	MID	*** MISSION DESCRIPTION TEXT ***							
SID1	TIME1	SID2	TIME2	SID3	TIME3	SID4	TIME4		CONT
SID5	TIME5								

Field	Contents
MID	Mission Identification number (integer)
SIDn	Segment Identification number of segment n (integer)
TIMEn	Flight time (hours) for segment n (real)

BLOCK -- A mission block is defined as a sequence of missions. Each mission is specified by the Mission ID (MID) and a number of sequential repetitions. The sequence of missions within the mission block follows the order of the input card. Therefore, if

the same mission occurs once in the beginning of the mission block and once near the end, it must be specified as two separate missions.

1	2	3	4	5	6	7	8	9	10
BLOCK	BID	MID1	NUM1	MID2	NUM2	MID3	NUM3		CONT
MID4	NUM4								

Field	Contents
BID	Mission Block Identification number (integer)
MIDn	Mission Identification number for mission n (integer)
NUMn	Number of times mission n is flown (integer)

FLIGHT -- A flight is defined as a sequence of mission blocks. Each mission block is specified by the Block ID (BID) and a number of sequential repetitions. The sequence of mission blocks within the flight follows the order of the input card. Typically, a flight consists of 1000 flight hours; however, this is only for the convenience of the user and there are no input restrictions concerning the number of flight hours per flight.

1	2	3	4	5	6	7	8	9	10
FLIGHT	FID	BID1	NUM1	BID2	NUM2	BID3	NUM3		CONT
BID4	NUM4								

Field	Contents
FID	Flight Identification number (integer)
BIDn	Mission Block Identification number for block n (integer)
NUMn	Number of times mission block n is flown (integer)

LIFE -- A life is defined as a sequence of flights. Each flight is specified by the Flight ID (FID) and a number of sequential repetitions. The sequence of flights within the aircraft life follows the order of the input card. The load history file defined by the sequence of flights can be repeated and/or each load cycle in the load history file can be blocked. Therefore, the total number of flight hours in the aircraft life is the sum of the flight hours in the flights multiplied by the repeating and blocking factors.

1	2	3	4	5	6	7	8	9	10
LIFE	REPEATING	BLOCKING	FID1	NUM1	FID2	NUM2	FID3	NUM3	CONT
FID4	NUM4								

Field	Contents
REPEATING	Number of times the load history file for the aircraft's life should be repeated (integer)
BLOCKING	Number of times each load cycle in the load history file for the aircraft's life should be blocked (integer)
FIDn	Flight Identification number for flight n (integer)
NUMn	Number of times flight n is flown (integer)

COMMENT -- Comment lines can be included in the input file to assist in the readability of the input. Any input line with an asterisk (*) in the first column is considered a comment line by the program. The comment line has no impact of program execution.

1	2	3	4	5	6	7	8	9	10
*									

END DATA -- This command must be placed at the end of the input file.

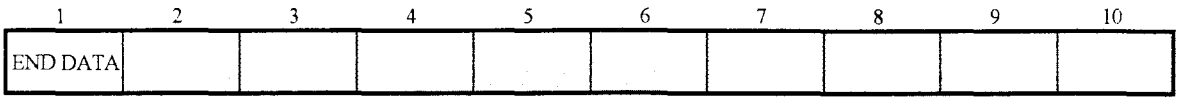

Sample Input File:

```
*2345678*2345678*2345678*2345678*2345678*2345678*2345678*2345678*2345678*2345678
LIFE          10        1        1       10
FLIGHT         1        1       10
BLOCK          1        1       10
MISSION        1                 *** CUMMULATIVE MISSION PROFILE ***
       1     1.0
SPECTRUM       1       EX        *** CUMMULATIVE SPECTRUM ***
      9.0      20      8.0      200      7.0     1000      6.0     7000          CONT
      5.0   20000      4.0    90000      3.0   200000      2.0   800000          CONT
      0.0    7000     -1.0      200     -2.0       10
SEGMENT2       1        1        0      103      105    0.111    1.000
SEGMENT2       1        1        1      103      105    1.000    0.500          CONT
      103      108    1.000    0.500
SEGMENT2       1        1        2      103      105    0.889    0.500          CONT
      103      108    0.889    0.500
SEGMENT2       1        1        3      103      105    0.778    0.500          CONT
      103      108    0.778    0.500
SEGMENT2       1        1        4      103      105    0.667    0.250          CONT
      103      108    0.667    0.250      103      107    1.000    0.250          CONT
      103      107    0.500    0.250
SEGMENT2       1        1        5      103      105    0.556    0.250          CONT
      103      108    0.556    0.250      103      107    0.833    0.250          CONT
      103      107    0.417    0.250
SEGMENT2       1        1        6      103      105    0.444    0.250          CONT
      103      108    0.444    0.250      103      107    0.667    0.250          CONT
      103      107    0.333    0.250
SEGMENT2       1        1        7      103      105    0.333    0.250          CONT
      103      108    0.333    0.250      103      107    0.500    0.250          CONT
      103      107    0.250    0.250
SEGMENT2       1        1        8      103      105    0.222    0.250          CONT
      103      108    0.222    0.250      103      107    0.333    0.250          CONT
      103      107    0.167    0.250
SEGMENT2       1        1        9      103      106    0.250    0.500          CONT
      103      109    0.500    0.125      103      109    0.250    0.125          CONT
      103      113    0.500    0.125      103      113    0.250    0.125
SEGMENT2       1        1       10      103      106    0.500    0.500          CONT
      103      109    1.000    0.125      103      109    0.500    0.125          CONT
      103      113    1.000    0.125      103      113    0.500    0.125
SEGMENT2       1        1       11      103      106    0.750    1.000
END DATA
```

Sample Ouput File:

```
 PANEL INPUT FILE:              load10.inp
 LOAD HISTORY FILE:             load10.dat


 DATA ECHO MODEL DEFINITION:

*2345678*2345678*2345678*2345678*2345678*2345678*2345678*2345678*2345678*234567
LIFE           10        1        1       10        0        0        0        0
FLIGHT          1        1       10        0        0        0        0
BLOCK           1        1       10        0        0        0        0
MISSION         1              *** CUMMULATIVE MISSION PROFILE ***
        1     1.0        0      0.0        0      0.0        0      0.0
SPECTRUM        1   EXCEED   *** CUMMULATIVE SPECTRUM ***
      9.0       20      8.0      200      7.0     1000      6.0     7000            CONT
      5.0    20000      4.0    90000      3.0   200000      2.0   800000            CONT
      0.0     7000     -1.0      200     -2.0       10      0.0        0
SEGMENT2        1        1        0      103      105 0.1E+00.100E+01
SEGMENT2        1        1        1      103      105 0.1E+01.500E+00            CONT
      103     108 0.1E+01.500E+00        0        0 0.0E+00.000E+00
SEGMENT2        1        1        2      103      105 0.9E+00.500E+00            CONT
      103     108 0.9E+00.500E+00        0        0 0.0E+00.000E+00
SEGMENT2        1        1        3      103      105 0.8E+00.500E+00            CONT
      103     108 0.8E+00.500E+00        0        0 0.0E+00.000E+00
SEGMENT2        1        1        4      103      105 0.7E+00.250E+00            CONT
      103     108 0.7E+00.250E+00      103      107 0.1E+01.250E+00            CONT
      103     107 0.5E+00.250E+00        0        0 0.0E+00.000E+00
SEGMENT2        1        1        5      103      105 0.6E+00.250E+00            CONT
      103     108 0.6E+00.250E+00      103      107 0.8E+00.250E+00            CONT
      103     107 0.4E+00.250E+00        0        0 0.0E+00.000E+00
SEGMENT2        1        1        6      103      105 0.4E+00.250E+00            CONT
      103     108 0.4E+00.250E+00      103      107 0.7E+00.250E+00            CONT
      103     107 0.3E+00.250E+00        0        0 0.0E+00.000E+00
SEGMENT2        1        1        7      103      105 0.3E+00.250E+00            CONT
      103     108 0.3E+00.250E+00      103      107 0.5E+00.250E+00            CONT
      103     107 0.3E+00.250E+00        0        0 0.0E+00.000E+00
SEGMENT2        1        1        8      103      105 0.2E+00.250E+00            CONT
      103     108 0.2E+00.250E+00      103      107 0.3E+00.250E+00            CONT
      103     107 0.2E+00.250E+00        0        0 0.0E+00.000E+00
SEGMENT2        1        1        9      103      106 0.3E+00.500E+00            CONT
      103     109 0.5E+00.125E+00      103      109 0.3E+00.125E+00            CONT
      103     113 0.5E+00.125E+00      103      113 0.3E+00.125E+00
SEGMENT2        1        1       10      103      106 0.5E+00.500E+00            CONT
      103     109 0.1E+01.125E+00      103      109 0.5E+00.125E+00            CONT
      103     113 0.1E+01.125E+00      103      113 0.5E+00.125E+00
SEGMENT2        1        1       11      103      106 0.8E+00.100E+01
END DATA


 DATA SUMMARY:

 FLIGHT        HOURS     # TIMES    TOTAL HRS # BLOCKS # MISSIONS # SEGMENTS
     1         100.0          10       1000.0       100         10         1


 TOTAL FLIGHT HOURS =    1000.00

 REPEATED      10 TIMES
 GRAND TOTAL FLIGHT HOURS =   10000.00


                          TOTAL                      AVERAGE PER 1000 HRS
   NZ          OCCURANCES       EXCEEDANCES       OCCURANCES       EXCEEDANCES
   10                 0.0               0.0              0.0               0.0
    9               200.0             200.0             20.0              20.0
    8              1800.0            2000.0            180.0             200.0
    7              8000.0           10000.0            800.0            1000.0
    6             60000.0           70000.0           6000.0            7000.0
    5            130000.0          200000.0          13000.0           20000.0
    4            700000.0          900000.0          70000.0           90000.0
    3           1100000.0         2000000.0         110000.0          200000.0
    2           6000000.0         8000000.0         600000.0          800000.0
    1                 0.0         8000000.0              0.0          800000.0
    0             68000.0           70000.0           6800.0            7000.0
   -1              1900.0            2000.0            190.0             200.0
   -2               100.0             100.0             10.0              10.0
   -3                 0.0               0.0              0.0               0.0
```

Appendix B: PANEL Program User's Guide

The PANEL program calculates the fatigue stress allowable for aircraft wing panels. This program uses the load history file created by the USAGE program in coordination with an ASTROS finite element model solution to create a stress history file for the wing panels. Using the stress history file, the fatigue analysis (performed by MODGRO) is iterated until convergence of the fatigue stress allowable. The PANEL program is executed via an UNIX script with the following command line syntax:

FRACTURE *input_filename load_history_file ASTROS_file ASTROS_password*

Field	Contents
input_filename	Filename of the PANEL input file (.inp)
load_history_file	Filename of the load history file created by the USAGE program (.dat)
ASTROS_file	ASTROS solution model file (.D01)
ASTROS_password	Password for the ASTROS model file

NOTE: The file extensions are not specified at the command line.

The results of the PANEL program are written to the default system output. In addition, the crack propagation (crack length vs. number of cycles) for each panel is written in tabular form to separate output files (*input_filename*_nn.dat, where nn is a counter). The PANEL program also creates several temporary files which are deleted upon completion of the program.

Input Format:

PANEL -- The PANEL command defines the panel in terms of a master element (QUAD4) in the ASTROS finite element model. In addition, the command points to a fatigue material properties card and a crack description card.

1	2	3	4	5	6	7	8	9	10
PANEL	PANELID	MATID	CRACKID						

Field	Contents
PANELID	Panel Identification number (Master Element number) (integer)
MATID	Fatigue Material Properties Identification number (integer)
CRACKID	Crack Description Identification number (integer)

PANELSET -- The PANELSET specifies the default values for the fatigue material properties card and a crack description card.

1	2	3	4	5	6	7	8	9	10
PANELSET		MATID	CRACKID						

Field	Contents
MATID	Fatigue Material Properties Identification number
CRACKID	Crack Description Identification number

FMAT1 -- This input card defines the material fatigue properties in terms of the Walker Equation.

1	2	3	4	5	6	7	8	9	10
FMAT1	MATID	KIC	RLO	RHI	YIELD	NUMSEG	*** DESCRIPTION TEXT ***		
WC1	N1	KCUT1							
WC2	N2	KCUT2							
. . .									
M	KITH								

Field	Contents
MATID	Fatigue Material Properties Identification number (integer)
KIC	Plain Strain Fracture Toughness (real)
RLO & RHI	The range of stress ratio, R, for which the fatigue data is valid (real)
YIELD	Yield Stress (real)
NUMSEG	The number of segments used to define the fatigue data. (integer) Each segment is defined by the Walker Equation: $\frac{da}{dN} = C\left(K_{\max}(1-R)^m\right)^n$
WCn	The Coefficient in the Walker Equation for segment n (real)
Nn	The fatigue slope in the Walker Equation for segment n (real)
KCUTn	The upper cut-off of stress intensity for segment n (real)
M	The exponent on the stress ratio term (1-R) (real)
KITH	Plain Strain Stress Intensity Threshold (real)

CRACK -- This input card defines the crack in the panel. If a user defined crack model is specified (1000 or 2000), then the Beta table is used to define stress intensity coefficient, β. For all other crack models, the Beta Table is used as a correction factor, $\beta_{correction}$, to the stress intensities calculated in MODGRO.

1	2	3	4	5	6	7	8	9	10
CRACK	CRACKID	MODEL	BETA_C	BETA_A	CRACK_C	CRACK_A	DIAM	RETARD	PARAM

Field	Contents
CRACKID	Crack Description Identification number (integer)
MODEL	MODGRO Crack Model number (integer)
BETA_C	Beta Table Identification number for the crack's major axis (integer) -- optional
BETA_A	Beta Table Identification number for the crack's minor axis (integer) -- optional
CRACK_C	Initial half-crack length in the crack's major axis (real)
CRACK_A	Initial half-crack length in the crack's minor axis (real)
DIAM	Hole Diameter for cracks emanating from a hole (real)
RETARD	Specifies the retardation model to be used (character): NO - no retardation W - Willenborg Retardation C - Closure model
PARAM	Parameter for the retardation model (real)

CRACKSET -- Defines the default values for the CRACK data card.

1	2	3	4	5	6	7	8	9	10
CRACKSET		MODEL	BETA_C	BETA_A	CRACK_C	CRACK_A	DIAM	RETARD	PARAM

Field	Contents
CRACKID	Crack Description Identification number (integer)
MODEL	MODGRO Crack Model number (integer)
BETA_C	Beta Table Identification number for the crack's major axis (integer) -- optional
BETA_A	Beta Table Identification number for the crack's minor axis (integer) -- optional
CRACK_C	Initial half-crack length in the crack's major axis (real)
CRACK_A	Initial half-crack length in the crack's minor axis (real)
DIAM	Hole Diameter for cracks emanating from a hole (real)
RETARD	Specifies the retardation model to be used (character): NO - no retardation W - Willenborg Retardation C - Closure model
PARAM	Parameter for the retardation model (real)

BETA -- This input card specifies a Beta Table (Beta vs. crack length).

1	2	3	4	5	6	7	8	9	10
BETA	BETAID	NUM							
C1	BETA1								
C2	BETA2								

Field	Contents
BETAID	Beta Table Identification number (integer)
NUM	Number of data points in the Beta Table (integer)

Cn	Crack length for the data point n (real)
BETAn	Beta for the data point n (real)

CRITERIA -- This data card is used to define the design criteria for the aircraft wing panels. The design criteria for wing panels is that the crack size must not exceed a specified value within a given time (specified as a multiplication factor of the aircraft's life).

1	2	3	4	5	6	7	8	9	10
CRITERIA	FACTOR	CRACK							

Field	Contents
FACTOR	Multiplication factor for the design usage (or life) of the panel (real)
CRACK	Maximum crack size (real) NOTE: Set to zero for critical crack length (i.e. fracture)

ITERATE -- This input card specifies the convergence criteria. The convergence criteria consists of an upper and lower tolerance on the design criteria. In addition, a maximum number of iterations can be specified.

1	2	3	4	5	6	7	8	9	10
ITERATE	LOWTOL	UPTOL	MAXITER						

Field	Contents
LOWTOL & UPTOL	Lower and Upper Tolerance on the convergence to the design criteria (real)
MAXITER	Maximum number of iterations (integer)

OVERRIDE -- This data card allows the panel's geometry data extracted from the ASTROS data file to be overridden. This override applies to all panels in the input file.

1	2	3	4	5	6	7	8	9	10
OVERRIDE	LENGTH	WIDTH	THICK						

Field	Contents
LENGTH	Panel Length (real)
WIDTH	Panel Width (real)
THICK	Panel Thickness (real)

COMMENT -- Comment lines can be included in the input file to assist in the readability of the input. Any input line with an asterisk (*) in the first column is considered a comment line by the program. The comment line has no impact of program execution.

1	2	3	4	5	6	7	8	9	10
*									

END DATA -- This command must be placed at the end of the input file.

1	2	3	4	5	6	7	8	9	10
END DATA									

Sample Input File:

```
*2345678*2345678*2345678*2345678*2345678*2345678*2345678*2345678*2345678*2345678
CRITERIA      2.0      0.0
ITERATE      0.02      0.0       20
CRACKSET                                                                 W      2.5
PANEL        2549        3        1
PANEL        2549        4        1
PANEL        2549        5        1
CRACK           1     2010        1             0.125
FMAT1           3     45.0     -3.0      1.0     66.0        1    ALUMINUM
 3.5E-10     3.42     45.0
    -0.3      4.0
FMAT1           4     45.0     -3.0      1.0     66.0        1    ALUMINUM
 3.5E-10     3.80     45.0
    -0.3      4.0
FMAT1           5     45.0     -3.0      1.0     66.0        1    ALUMINUM
 3.5E-10     4.18    45.0
    -0.3      4.0
*
*  h/b=0.5   b=12
BETA            1       15
   0.000    1.000
   0.600    1.015
   1.200    1.045
   1.800    1.100
   2.400    1.180
   3.000    1.270
   3.600    1.370
   4.200    1.480
   4.800    1.605
   5.400    1.755
   6.000    1.930
   6.600    2.160
   7.200    2.410
   7.800    2.700
   8.400    3.05
END DATA
```

Sample Output File:

```
 PANEL INPUT FILE:            lenwid.inp
 LOAD HISTORY FILE:           load10.dat


 DATA ECHO MODEL DEFINITION:

*2345678*2345678*2345678*2345678*2345678*2345678*2345678*2345678*2345678*234567
CRITERIA 0.2E+01 0.0E+00
ITERATE  0.0E+00 2.0E-02       20
CRACKSET               0        0        0 0.0E+00 0.0E+00 0.0E+00     W   2.5E+00
PANEL         2549        3        1
PANEL         2549        4        1
PANEL         2549        5        1
CRACK            1     2010        1        0 1.2E-01 0.0E+00 0.0E+00     W   2.5E+00
FMAT1            3 4.5E+01-3.0E+00 1.0E+00 6.6E+01        1
 3.5E-10 3.4E+00 4.5E+01
-3.0E-01 4.0E+00
FMAT1            4 4.5E+01-3.0E+00 1.0E+00 6.6E+01        1
 3.5E-10 3.8E+00 4.5E+01
-3.0E-01 4.0E+00
FMAT1            5 4.5E+01-3.0E+00 1.0E+00 6.6E+01        1
 3.5E-10 4.2E+00 4.5E+01
-3.0E-01 4.0E+00
*
*  h/b=0.5  b=12
BETA             1       15
 0.0E+00 1.0E+00
 6.0E-01 1.0E+00
 1.2E+00 1.0E+00
 1.8E+00 1.1E+00
 2.4E+00 1.2E+00
 3.0E+00 1.3E+00
 3.6E+00 1.4E+00
 4.2E+00 1.5E+00
 4.8E+00 1.6E+00
 5.4E+00 1.8E+00
 6.0E+00 1.9E+00
 6.6E+00 2.2E+00
 7.2E+00 2.4E+00
 7.8E+00 2.7E+00
 8.4E+00 3.0E+00
END DATA
```

```
****************************************
*  PANEL =    1     ELEMENT ID =   2549  *
****************************************


PANEL GEOMETRY:
  LENGTH =    13.00
  WIDTH =    24.00
  THICKNESS =   0.3800


CRACK GEOMETRY:
  MODEL NUMBER = 2010
  CRACK LENGTH (MAJOR AXIS) =    0.1250
  CRACK LENGTH (MINOR AXIS) =    0.0000
  HOLE DIAMETER =    0.0000


******  STRESS REPORT  ******


TOTAL FLIGHT HOURS =    10000.0
TOTAL NUMBER OF STRESS CYLCES =        7999980
   NUMBER OF STRESS CYCLES IN STRESS HISTORY =     799998
   NUMBER OF TIMES EACH STRESS CYCLE IS REPEATED (BLOCKED) =     1
   NUMBER OF TIMES THE STRESS HISTORY FILE IS REPEATED =    10
```

	TOTAL		AVERAGE PER 1000 HRS	
%MAX	OCCURANCES	EXCEEDANCES	OCCURANCES	EXCEEDANCES
1.0	90	90	9	9
0.9	0	90	0	9
0.8	900	990	90	99
0.7	4990	5980	499	598
0.6	19000	24980	1900	2498
0.5	62500	87480	6250	8748
0.4	240000	327480	24000	32748
0.3	625000	952480	62500	95248
0.2	2097500	3049980	209750	304998
0.1	11380020	14430000	1138002	1443000
0.0	1559730	15989730	155973	1598973
-0.1	9910	10230	991	1023
-0.2	90	320	9	32
-0.3	230	230	23	23
-0.4	0	0	0	0
-0.5	0	0	0	0
-0.6	0	0	0	0
-0.7	0	0	0	0
-0.8	0	0	0	0
-0.9	0	0	0	0
-1.0	0	0	0	0

```
LARGEST MAXIMUM PRINCIPAL STRESS = 32078.7
AVERAGE ANGLE OF MAXIMUM PRINCIPAL STRESS = -1.5


DESIGN CRITERIA:
  LIFE MULTIPLICATION FACTOR =    2.000
  CRACK LENGTH =    0.000     (ZERO IF CRITERIA IS FRACTURE)

CONVERGENCE CRITERIA:
  NUMBER OF CYCLES =  15999960
  UPPER TOLERANCE = 0.00%
  LOWER TOLERANCE = 2.00%
  MAXIMUM NUMBER OF ITERATIONS =  20
```

ITERATION	STRESS	CYCLES	CRACKSIZE
1	33.000	1830451	0.596
2	19.192	11560767	1.505
3	17.495	16183221	1.743
4	17.559	16001618	1.743
5	17.579	15925628	1.742

```
CONVERGED TO WITHIN  0.46% OF CRITERIA AT SMF =    17.579
```

```
****************************************
*  PANEL =    2     ELEMENT ID =  2549  *
****************************************


PANEL GEOMETRY:
  LENGTH =    13.00
  WIDTH =    24.00
  THICKNESS =  0.3800


CRACK GEOMETRY:
  MODEL NUMBER = 2010
  CRACK LENGTH (MAJOR AXIS) =    0.1250
  CRACK LENGTH (MINOR AXIS) =    0.0000
  HOLE DIAMETER =    0.0000


******  STRESS REPORT  ******


TOTAL FLIGHT HOURS =    10000.0
TOTAL NUMBER OF STRESS CYLCES =        7999980
   NUMBER OF STRESS CYCLES IN STRESS HISTORY =     799998
   NUMBER OF TIMES EACH STRESS CYCLE IS REPEATED (BLOCKED) =     1
   NUMBER OF TIMES THE STRESS HISTORY FILE IS REPEATED =    10
```

	TOTAL		AVERAGE PER 1000 HRS	
%MAX	OCCURANCES	EXCEEDANCES	OCCURANCES	EXCEEDANCES
1.0	90	90	9	9
0.9	0	90	0	9
0.8	900	990	90	99
0.7	4990	5980	499	598
0.6	19000	24980	1900	2498
0.5	62500	87480	6250	8748
0.4	240000	327480	24000	32748
0.3	625000	952480	62500	95248
0.2	2097500	3049980	209750	304998
0.1	11380020	14430000	1138002	1443000
0.0	1559730	15989730	155973	1598973
-0.1	9910	10230	991	1023
-0.2	90	320	9	32
-0.3	230	230	23	23
-0.4	0	0	0	0
-0.5	0	0	0	0
-0.6	0	0	0	0
-0.7	0	0	0	0
-0.8	0	0	0	0
-0.9	0	0	0	0
-1.0	0	0	0	0

```
LARGEST MAXIMUM PRINCIPAL STRESS = 32078.7
AVERAGE ANGLE OF MAXIMUM PRINCIPAL STRESS = -1.5


DESIGN CRITERIA:
  LIFE MULTIPLICATION FACTOR =   2.000
  CRACK LENGTH =    0.000     (ZERO IF CRITERIA IS FRACTURE)

CONVERGENCE CRITERIA:
  NUMBER OF CYCLES =  15999960
  UPPER TOLERANCE = 0.00%
  LOWER TOLERANCE = 2.00%
  MAXIMUM NUMBER OF ITERATIONS =  20
```

ITERATION	STRESS	CYCLES	CRACKSIZE
1	33.000	730772	0.596
2	15.256	13623851	2.119
3	14.661	16168365	2.224
4	14.703	15871512	2.224

```
CONVERGED TO WITHIN  0.80% OF CRITERIA AT SMF =    14.703
```

```
**************************************
*  PANEL =   3    ELEMENT ID =  2549  *
**************************************


PANEL GEOMETRY:
  LENGTH =   13.00
  WIDTH =   24.00
  THICKNESS =  0.3800


CRACK GEOMETRY:
  MODEL NUMBER = 2010
  CRACK LENGTH (MAJOR AXIS) =   0.1250
  CRACK LENGTH (MINOR AXIS) =   0.0000
  HOLE DIAMETER =   0.0000


******  STRESS REPORT  ******


TOTAL FLIGHT HOURS =   10000.0
TOTAL NUMBER OF STRESS CYLCES =       7999980
   NUMBER OF STRESS CYCLES IN STRESS HISTORY =    799998
   NUMBER OF TIMES EACH STRESS CYCLE IS REPEATED (BLOCKED) =    1
   NUMBER OF TIMES THE STRESS HISTORY FILE IS REPEATED =   10
```

	TOTAL		AVERAGE PER 1000 HRS	
%MAX	OCCURANCES	EXCEEDANCES	OCCURANCES	EXCEEDANCES
1.0	90	90	9	9
0.9	0	90	0	9
0.8	900	990	90	99
0.7	4990	5980	499	598
0.6	19000	24980	1900	2498
0.5	62500	87480	6250	8748
0.4	240000	327480	24000	32748
0.3	625000	952480	62500	95248
0.2	2097500	3049980	209750	304998
0.1	11380020	14430000	1138002	1443000
0.0	1559730	15989730	155973	1598973
-0.1	9910	10230	991	1023
-0.2	90	320	9	32
-0.3	230	230	23	23
-0.4	0	0	0	0
-0.5	0	0	0	0
-0.6	0	0	0	0
-0.7	0	0	0	0
-0.8	0	0	0	0
-0.9	0	0	0	0
-1.0	0	0	0	0

```
LARGEST MAXIMUM PRINCIPAL STRESS = 32078.7
AVERAGE ANGLE OF MAXIMUM PRINCIPAL STRESS = -1.5


DESIGN CRITERIA:
  LIFE MULTIPLICATION FACTOR =   2.000
  CRACK LENGTH =   0.000     (ZERO IF CRITERIA IS FRACTURE)

CONVERGENCE CRITERIA:
  NUMBER OF CYCLES =  15999960
  UPPER TOLERANCE = 0.00%
  LOWER TOLERANCE = 2.00%
  MAXIMUM NUMBER OF ITERATIONS =  20
```

ITERATION	STRESS	CYCLES	CRACKSIZE
1	33.000	284149	0.597
2	12.047	22361329	2.841
3	13.045	14103579	2.576
4	12.885	14915573	2.576
5	12.828	15257256	2.575
6	12.800	15910704	2.575

```
CONVERGED TO WITHIN  0.56% OF CRITERIA AT SMF =    12.800


ALL PANELS COMPLETED
```

Bibliography

1. Neill, D.J., E.H. Johnson, and D.L. Herendeen. Automated Structural Optimization System (ASTROS), AFWAL-TR-88-3028, April 1988.
2. Venkayya, V.B. "Structural Optimization: Local Issues in Global Modeling," International Symposium on Aerospace Sciences and Engineering, Indian Institute of Science. Bangalore, India, 1992.
3. Gallegher, J.P., F.J. Giessler, A.P. Berens, and others. USAF Damage Tolerant Design Handbook: Guidelines for the Analysis and Design of Damage Tolerant Aircraft Structures, AFWAL-TR-82-3073 Rev B, 1984.
4. Aircraft Structural Integrity Program, Airplane Requirements, MIL-STD-1530, Aeronautical Systems Division, Wrigth-Patterson Air Force Base, OH, Sep 1972.
5. Airplane Damage Tolerance Requirements, MIL-A-83444, Air Force Aeronautical Systems Division, Wright-Patterson Air Force Base, OH, July 1974.
6. Airplane Strength and Rigidity Ground Tests, MIL-A-008867B, Air Force Aeronautical Systems Division, Wright-Patterson Air Force Base, OH, Aug 1975.
7. Owen, D.R. and A.J. Fawkes. Engineering Fracture Mechanics: Numerical Methods and Applications, Pinridge Press Ltd., Swansea, U.K.
8. Broek, David. Elementary Engineering Fracture Mechanics, Fourth Edition, Kluwar Academic Publishers, Dordrecht, Netherlands, 1991.
9. Kies, J.A., J.M. Krafft, R.J. Sanford and others. "Historical Note on the Development of Fracture Mechanics by G.R. Irwin," in Linear Fracture Mechanics, Ed. G.C. Sih, et. al., Envo Publishing Co., Bethlehem, PA, 1975.
10. Hardrath, Herbert F. "Fatigue and Fracture Mechanics," in Journal of Aircraft Vol 8, March 1971.
11. Tada, Hiroshi, Paul C. Paris, and George R. Irwin. The Stress Analysis of Cracks Handbook, Del Research Corporation, St. Louis, Missouri, 1978.
12. Rooke, D.P. and D.J. Cartwright. Compendium of Stress Intensity Facotrs, The Hillingdon Press, Uxbridge, England, 1973.
13. Trent, D.J. and I. Bouton. "Application of the Residual Strength Concept to Fatigue Design Criteria," in Proceedings of the Air Force Conference on Fatigue and Fracture of Aircraft Structures and Materials, AFFDL-TR-70-144.
14. McEvily, Aurther J. and Kunori Minakawa. "Crack Closure and Variable-Amplitude Fatigue Crack Growth," in Basic Questions in Fatigue Volume I, Ed. Jeffrey T. Fong and Richard J. Fields. Philadelphia, PA: ASTM Publications, 1988.
15. Saff, Charles R. "Crack Growth of Retardation and Acceleration Models," in Damage Tolerance of Metallic Structures: Analysis and Methods and Applications. Ed. James B. Chang and James L. Rudd. Philadelphia, PA: ASTM Publication, 1981.

16. Rudd, James L. "Air Force Damage Tolerance Design Philosophy," in Damage Tolerance of Metallic Structures: Analysis Methods and Applications. Ed. James B. Chang and James L. Rudd. Philadelphia, PA: ASTM Publications, 1981.

17. Morrison, Col. Harry B. "Aircraft Structural Integrity Program in AFLC," in Proceedings of the Air Force Conference on Fatigue and Fracture of Aircraft Structures and Materials, AFFDL-TR-70-144.

18. Glessler, Joseph, Seth Duell and Robert Cook. Handbook of Guidelines for the Development of Design Usage and Environmental Sequences for USAF Aircraft, AFWAL-TR-80-3156, 1980.

19. Rich, Daniel L., R.E. Pinckert and T.F. Christian. "Fatigue and Fracture Mechanics Analysis of Compression Loaded Aircraft Structure," in Case Histories Involving Fatigue & Fracture Machnics, Ed. C. Michael Hudson and Thomas P. Rich. Philadelphia, PA: ASTM Publications, March 1985.

20. Poe, C.C. "The Effect of Riveted and Uniformly Spaced Stringers on the Stress Intensity Factor of a Cracked Sheet," in Proceedings of the Air Force Conference on Fatigue and Fracture of Aircraft Structures and Materials, AFFDL-TR-70-144.

21. Swift, Thomas. "Fracture Analysis of Stiffened Structure," in Damage Tolerance of Metallic Structures: Analysis Methods and Applications. Ed. James B. Chang and James L. Rudd. Philadelphia, PA: ASTM Publications, 1981.

22. Denyer, Anthony G. "Aircraft Structural Maintenance Recommendations Based on Fracture Mechanics Analysis," in Case Histories Involving Fatigue & Fracture Mechanics. Ed. Michael C. Hudson and Thomas P. Rich. Philadelphia, PA: ASTM Publications, March 1985.

23. Harter, Jim. "Damage Tolerance Management of the X-29 Vertical Fin," in Advisory Group for Aerospace Research & Development Report 797, 1993.

24. Harter, James A. MODGRO: User's Manual, AFEAL-TM-88-157-FIBE, 1988.

25. Neil, D.J., E.H. Johnson and R.L. Hoesly. Automated Structural Optimization System (ASTROS): Volume IV - Programmer's Manual, AFWAL-TR-88-3028 Vol IV, July 1988.

26. Love, M.H., D.K. Barker and J.D. Bohlmann. An Aircraft Design Application Using ASTROS, WL-TR-93-3037, June 1993.

27. Boyer, Howard. Atlas of Fatigue Curves, American Society for Metals, Ohio, 1986.

28. Blair, Max and Greg Reich. "Aerospace Geometric Design with Pro/ENGINEER." Wright Laboratory, Flight Dynamics Directorate, Briefing slides data 4 Oct 1994.

Vita

Capt Clifton D. Nees [redacted]. He was raised in Cincinnati, Oh where he graduated from Moeller High School in 1983. He attended Iowa State University in Ames, Iowa on a four-year Air Force ROTC scholarship. He graduated with a Bachelor of Science degree in Mechanical Engineering. On 21 May 1988, he was commissioned as an officer in the USAF. His first assignment was at Eglin AFB, FL as a Loads Engineer in the 3246th Test Wing. His second position at Eglin AFB was as a technical program manager in the Wright-Laboratory, Armament Directorate. In June 1994, he entered the School of Engineering at the Air Force Institute of Technology.

REPORT DOCUMENTATION PAGE

Form Approved
OMB No. 0704-0188

1. AGENCY USE ONLY *(Leave blank)*	2. REPORT DATE	3. REPORT TYPE AND DATES COVERED
	Dec 1995	Master's Thesis

4. TITLE AND SUBTITLE
METHODOLOGY FOR IMPLEMENTING FRACTURE MECHANICS IN GLOBAL STRUCTURAL DESIGN OF AIRCRAFT

5. FUNDING NUMBERS

6. AUTHOR(S)
Clifton D. Nees, Captain, USAF

7. PERFORMING ORGANIZATION NAME(S) AND ADDRESS(ES)
Air Force Institute of Technology, WPAFB, OH 45433

8. PERFORMING ORGANIZATION REPORT NUMBER
AFIT/GAE/ENY/95D-18

9. SPONSORING / MONITORING AGENCY NAME(S) AND ADDRESS(ES)
Dr. Venkayya
WL/FIBA
Wright-Patterson AFB, OH 45433-7542

10. SPONSORING / MONITORING AGENCY REPORT NUMBER

11. SUPPLEMENTARY NOTES

12a. DISTRIBUTION / AVAILABILITY STATEMENT
Approved for public release; distribution unlimited

12b. DISTRIBUTION CODE

13. ABSTRACT *(Maximum 200 words)*

The analysis and design criteria of fracture mechanics are investigated for implementation with the Automated Structural Optimization System (ASTROS) global optimization design tool. The main focus is the optimal design of aircraft wing panels by applying fracture mechanics design criteria within the global finite element model. This effort consists of four main phases: investigation of fracture mechanics analysis methods and design criteria, formulation of a computational technique for damage tolerance design consistent with global optimization requirements, integration of the technique into the ASTROS design tool, and demonstration of the results.

14. SUBJECT TERMS
Fracture Mechanics, Fatigue, Damage Tolerance, Aircraft Optimization, Wing Panel Design, Local Modeling, Global Modeling

15. NUMBER OF PAGES
122

16. PRICE CODE

17. SECURITY CLASSIFICATION OF REPORT	18. SECURITY CLASSIFICATION OF THIS PAGE	19. SECURITY CLASSIFICATION OF ABSTRACT	20. LIMITATION OF ABSTRACT
Unclassified	Unclassified	Unclassified	UL

GENERAL INSTRUCTIONS FOR COMPLETING SF 298

The Report Documentation Page (RDP) is used in announcing and cataloging reports. It is important that this information be consistent with the rest of the report, particularly the cover and title page. Instructions for filling in each block of the form follow. It is important to ***stay within the lines*** to meet ***optical scanning requirements***.

Block 1. Agency Use Only *(Leave blank)*.

Block 2. Report Date. Full publication date including day, month, and year, if available (e.g. 1 Jan 88). Must cite at least the year.

Block 3. Type of Report and Dates Covered. State whether report is interim, final, etc. If applicable, enter inclusive report dates (e.g. 10 Jun 87 - 30 Jun 88).

Block 4. Title and Subtitle. A title is taken from the part of the report that provides the most meaningful and complete information. When a report is prepared in more than one volume, repeat the primary title, add volume number, and include subtitle for the specific volume. On classified documents enter the title classification in parentheses.

Block 5. Funding Numbers. To include contract and grant numbers; may include program element number(s), project number(s), task number(s), and work unit number(s). Use the following labels:

C	- Contract	**PR**	- Project
G	- Grant	**TA**	- Task
PE	- Program Element	**WU**	- Work Unit Accession No.

Block 6. Author(s). Name(s) of person(s) responsible for writing the report, performing the research, or credited with the content of the report. If editor or compiler, this should follow the name(s).

Block 7. Performing Organization Name(s) and Address(es). Self-explanatory.

Block 8. Performing Organization Report Number. Enter the unique alphanumeric report number(s) assigned by the organization performing the report.

Block 9. Sponsoring/Monitoring Agency Name(s) and Address(es). Self-explanatory.

Block 10. Sponsoring/Monitoring Agency Report Number. *(If known)*

Block 11. Supplementary Notes. Enter information not included elsewhere such as: Prepared in cooperation with...; Trans. of...; To be published in.... When a report is revised, include a statement whether the new report supersedes or supplements the older report.

Block 12a. Distribution/Availability Statement. Denotes public availability or limitations. Cite any availability to the public. Enter additional limitations or special markings in all capitals (e.g. NOFORN, REL, ITAR).

- **DOD** - See DoDD 5230.24, "Distribution Statements on Technical Documents."
- **DOE** - See authorities.
- **NASA** - See Handbook NHB 2200.2.
- **NTIS** - Leave blank.

Block 12b. Distribution Code.

- **DOD** - Leave blank.
- **DOE** - Enter DOE distribution categories from the Standard Distribution for Unclassified Scientific and Technical Reports.
- **NASA** - Leave blank.
- **NTIS** - Leave blank.

Block 13. Abstract. Include a brief *(Maximum 200 words)* factual summary of the most significant information contained in the report.

Block 14. Subject Terms. Keywords or phrases identifying major subjects in the report.

Block 15. Number of Pages. Enter the total number of pages.

Block 16. Price Code. Enter appropriate price code *(NTIS only)*.

Blocks 17. - 19. Security Classifications. Self-explanatory. Enter U.S. Security Classification in accordance with U.S. Security Regulations (i.e., UNCLASSIFIED). If form contains classified information, stamp classification on the top and bottom of the page.

Block 20. Limitation of Abstract. This block must be completed to assign a limitation to the abstract. Enter either UL (unlimited) or SAR (same as report). An entry in this block is necessary if the abstract is to be limited. If blank, the abstract is assumed to be unlimited.

★U.S.GPO:1993-0-336-043